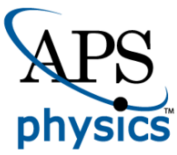

Opportunities at the Frontiers of Spintronics

Axel Hoffmann and Sam D. Bader

Phys. Rev. Applied **4**, 047001 — Published 5 October 2015

DOI: 10.1103/PhysRevApplied.4.047001

New Opportunities at the Frontiers of Spintronics

Axel Hoffmann and Sam D. Bader

Materials Science Division, Argonne National Laboratory, Argonne, IL 60439

Abstract

The field of spintronics, or magnetic electronics, is maturing and giving rise to new subfields. These new directions involve the study of collective spin excitations and couplings of the spin system to additional degrees of freedom of a material, as well as metastable phenomena due to perturbations that drive the system far from equilibrium. The interactions lead to possibilities for future applications within the realm of energy-efficient information technologies. Examples discussed herein include research opportunities associated with (i) various spin-orbit couplings, such as spin Hall effects, (ii) couplings to the thermal bath of a system, such as in spin Seebeck effects, (iii) spin-spin couplings, such as via induced and interacting magnon excitations, and (iv) spin-photon couplings, such as in ultra-fast magnetization switching due to coherent photon pulses. These four basic frontier areas of research are giving rise to new applied disciplines known as spin-orbitronics, spin-caloritronics, magnonics, and spin-photonics, respectively. These topics are highlighted in order to stimulate interest in the new directions that spintronics research is taking, and to identify open issues to pursue.

I. Introduction

The discovery of giant magnetoresistance [1,2] was the genesis for the field of spintronics, which focuses on the interplay between charge transport and magnetization structure and dynamics [3,4]. Spintronics is a remarkable success story in terms of transitioning fundamental science into applications, since within a decade after its initial discovery giant magnetoresistance became an integral part of read heads in magnetic data storage enabling ever increasing amounts of digital data to be stored. As such, spintronics was instrumental in the digital revolution, wherein analog information was essentially replaced by digital data [5] to the point where the transmission, manipulation and storage of information have become a pervasive aspect of our lives.

While the initial applied impact of spintronics was mostly related to information storage, which already utilized magnetic materials for long-term data retention, more recently there have been increased efforts to integrate spintronic concepts also into the logic operations of information technologies. The driver for this is that continuous miniaturization of semiconducting electronics, known as "Moore's law", goes hand in hand with increased power dissipation due to leakage currents [6]. Towards this end, information-processing systems based on magnetic degrees of freedom offer appealing opportunities. Unlike purely charge-based systems, information encoded in magnetization states is generally non-volatile, thus reducing the power requirement for maintaining data. However, it should be noted that with decreasing size thermal stability (and thus volatility) becomes an issue that may require materials with increased magnetic anisotropies [7] in order to develop

magnetic devices with ultra-high miniaturization. Nevertheless, since the energy difference between opposite magnetization directions can be negligibly small, this offers, in principle, the possibility to manipulate data at its thermodynamic limits [8]. Besides overcoming the power dissipation limitations of semiconducting electronics, improved energy-efficient information technologies are also imperative for overcoming the concomitant increasing global energy consumption, which is driven, in part, by the ubiquitous growth in popularity of electronic devices [9].

The aim of this review is to briefly summarize recent key novel developments to understand fundamental phenomena within the field of spintronics, which are poised to also impact applications. For this purpose we focus on four topics: spin-orbitronics, spin-caloritronics, magnonics, and ultrafast spin-photonics. These examples illustrate some of the complexity encountered due to the inherent mesoscale nature of magnetism, where interactions at many different length-scales are relevant and lead to the coupling of many different degrees of freedom [10]. Spin-orbitronics is an emergent subfield of spintronics, which aims at harnessing spin-orbit coupling for the generation and detection of spin currents even in non-magnetic materials. Phenomena driven by spin-orbit coupling were also essential in establishing the new research direction of spin caloritronics, which is focused on the interplay of spin- and charge-currents with heat-currents. Spin wave excitations (magnons) appear to be important for understanding heat-driven phenomena, but also form the basis of the new spintronics concept known as magnonics. Here the goal is to use magnons instead of diffusive spin currents to encode and process information. While spin wave excitations range in frequencies from the GHz-to-THz

range, it was recently realized that magnetization dynamics can also occur at time-scales that go beyond the typical frequencies of spin wave excitations. This is known as ultrafast light-pulse-triggered magnetization phenomena, or spin-photonics. Their investigation has opened up new ways to explore the interaction between magnetism and light. It is important to note that this review does not intend to be a comprehensive overview of all recent spintronic developments. There are other promising opportunities beyond the topics covered herein. Given the breadth of interests of the applied magnetism community [11] and the brevity of this review, it is unavoidable that the selection of these topics and the examples provided for illustrating them are subjective and driven by the research interests of the authors.

II. Spin-Orbitronics

For the first decade after the discovery of giant magnetoresistance [1,2] virtually all spintronic concepts were based on the idea of generating a spin-polarized current by passing a charge current through a ferromagnetic layer [4]. More recently it has been realized that spin-orbit interactions can provide an efficient alternative pathway for generating spin currents from charge current flows even through non-magnetic conductors. Among the key phenomena are spin Hall effects [12,13], which were already theoretically predicted in 1971 by D'yakonov and Perel' [14]. Here either extrinsic spin-dependent scattering or intrinsic spin dependent transverse velocities determined by the electronic band structure can convert an initially unpolarized charge current into a transverse spin current, which leads to

spin accumulation at the boundaries of the conductors. Such spin Hall effects initially were considered mostly an academic curiosity. However, recently it was realized that the spin currents can rival or even exceed those generated by direct electric injection, which occurs upon passing a charge current from a ferromagnetic layer with spin-polarized charge transport through an interface into an adjacent non-magnetic conductor. Naïvely this seems surprising, since using either a half-metallic ferromagnetic injector [15] or symmetry selective tunnel-junctions, such as MgO [16–18], can result in charge current polarizations close to an ideal 100%. In contrast, for bulk spin Hall effects, the materials-specific spin Hall angle, given by the ratio of charge-to-spin current densities, is the parameter that describes the conversion efficiencies. For the best-known materials the parameter reaches values of 10–30% [13,19–24]. However, due to the transverse nature of spin Hall effects, the ratio of spin-to-charge current can actually exceed unity, since the cross section for the spin current can be significantly larger than the cross section for charge currents. In other words the same electron carrying the charge current can repeatedly transfer its spin angular momentum at opposite interfaces. For example, using a tunnel junction, where the free layer of the tunnel junction is in contact to a conducting layer with large spin Hall effects (see Fig. 1) Liu *et al.* demonstrated that the spin Hall angle in Ta is sufficiently large to switch the magnetization of the free ferromagnetic layer [20]. From the measurements one can determine a spin Hall angle of 12%. But given the geometry of the sample, with the free layer being 100-nm wide and the Ta layer being 6-nm thick, the spin current absorbed in the free layer is about twice as large as the charge current flowing underneath the free layer,

ignoring any current shunting. For injection of spin currents into more extended structures, this ratio can become arbitrarily large, which indicates that spin Hall effects can have significant applied advantages as a source for spin currents. In addition, it has recently been realized that sizeable spin Hall effects may also exist in magnetically ordered materials and that the direction and magnitude of the magnetization may manipulate the spin Hall conductivities [25–29].

Furthermore, the transverse geometry enables spin current injection into insulators, such as yttrium iron garnet [30], and can result in a reduction of damping [31–33], and even in the excitation of auto-oscillations [34]. Similar auto-oscillation has also been observed in hetero-structures with metallic ferromagnets [35–37]. More recently it has also been shown that spin Hall effects can be used for the generation and detection of ferromagnetic resonance in insulators [38,39].

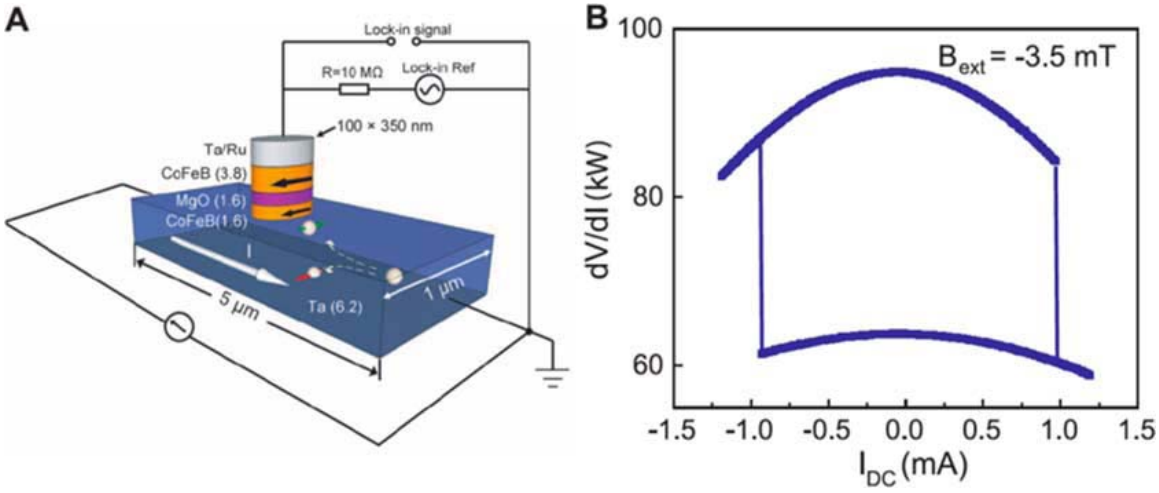

Fig. 1: (a) Three terminal device used for demonstrating magnetization switching via spin Hall effects. By passing a current through the extended Ta layer, a spin accumulation is generated via the spin Hall effect at the bottom interface with the free layer of a CoFeB/MgO/CoFeB tunnel junction stack. (b) Switching can then be

detected by monitoring the tunnel junction resistance. During the measurement an external field is applied to compensate the dipolar coupling between the free and fixed layers. Adapted from [20]. Reprinted with permission from AAAS.

The idea that the transverse geometry of spin Hall effects offers advantages for scaling devices by reducing the layer thickness of the charge-current-carrying layer is limited for bulk spin Hall effects by the spin diffusion length. Fortunately, a large spin Hall angle generally also is accompanied by a short spin diffusion length, typically of a few nm [22,40–43]. But this concept can be pushed to the ultimate limit by passing the charge current through a two-dimensional system, which can generate a current-induced spin accumulation. This has been theoretically established for the case of Rashba spin-orbit coupling [44,45] and recently it has been shown experimentally that Rashba states at metallic interfaces can result in significant spin-transfer torques [46]. It also was demonstrated for semiconductors that Rashba spin-orbit coupling leads to magnetization switching with electric currents [47]. More recently this has been extended to topological insulators [48,49], where strong Rashba-type spin-orbit coupling can give rise to metallic surface states for bulk insulators. Combining these materials with ferromagnetic layers enables the direct detection of the current-induced spin polarization, which is due to the spin-momentum locking given by the Rashba-type spin-orbit coupling [50]. This in turn results in a sizable spin-orbit torque on the ferromagnetic magnetization [51], which even can be used to switch the magnetization [52].

Just as the transverse geometry of spin Hall effects enables the generation of large spin currents from charge currents, it also lends itself for a careful metrology of these effects using macroscopically generated spin currents. The later can be achieved via spin pumping, which occurs when ferromagnetic resonance is excited in a ferromagnet in direct contact with a non-magnetic conductor, as schematically shown in Fig. 2(a) [53,54]. The magnetization dynamics at the interface gives rise to time- and spin-dependent scattering at the interface, which in turn generates a spin current in the non-magnetic conductor diffusing away from the interface. This spin current subsequently can be converted into a charge current via the inverse spin Hall effect [55–57]. Unlike electric spin-injection, which is typically limited to electrical contacts with small contact areas in order to avoid complications of inhomogeneous current flow, such as current crowding, spin pumping can be used to generate spin currents over arbitrarily large interfacial areas. This then enables the generation of macroscopic spin currents, which can be converted into relatively large electric voltages. As an example, Fig. 2(b) shows spin pumping/spin Hall effect voltages measured for a bilayer of 15-nm permalloy (Py) and 15-nm Pt measured at 4 GHz. The voltage spectrum contains two contributions, which can be separated by their symmetry: an antisymmetric Lorentzian contribution, which comes from the anisotropic magneto-resistance, and a symmetric Lorentzian contribution from the inverse spin Hall effect. The lateral length of this sample is 2.92 mm, which generates a voltage due to the spin Hall effect of about 0.5 mV. Measuring the spin Hall voltage as a function of non-magnetic layer thickness yields the spin diffusion length [22,58], and together with determining the spin current from the precession

cone angle of the ferromagnetic resonance, this permits the spin Hall angles to be determined; *i.e.,* the measurements on Py/Pt in Fig. 2(b) yield a spin Hall angle of 8.6±0.5% [22].

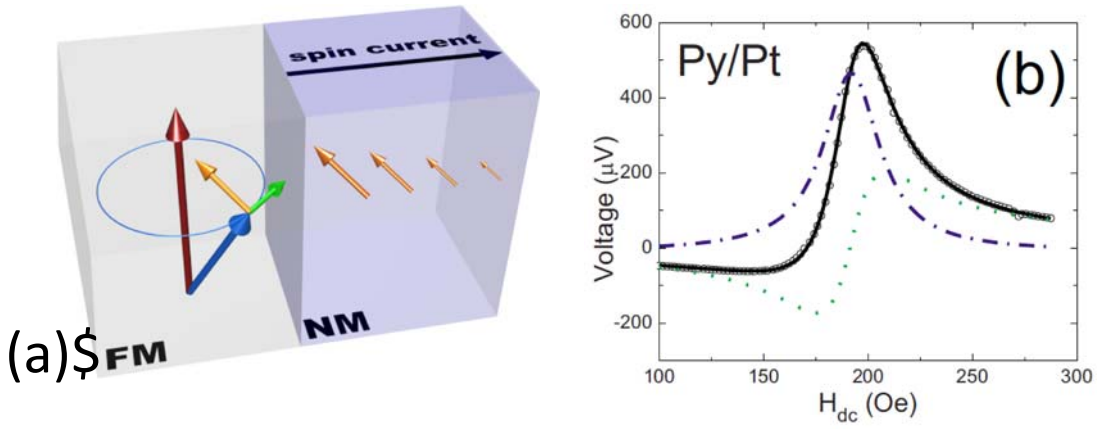

Fig. 2: (a) Schematic of a spin current generated in a non-magnetic metal (NM) via the magnetization precession in an adjacent ferromagnet (FM). (b) Voltage spectrum measured at 4 GHz in a spin pumping/inverse spin Hall effect measurement for a permalloy (Py)/Pt bilayer. The lineshape of the voltage as a function of a magnetic field has symmetric and antisymmetric Lorentzian components, which correspond to voltages generated by the spin Hall effect and the anisotropic magnetoresistance, respectively. Reprinted figure with permission from [59]. Copyright 2010 by the American Physical Society.

The relative ease of sample fabrication for spin-pumping experiments makes this approach well suited to investigate spin currents in a wide variety of materials. Besides measuring spin Hall effects in non-magnetic conductors, this approach has also been adopted for magnetically ordered systems, such as ferromagnets [26] and antiferromagnets [28]. In addition, it has been shown that induced magnetic

moments from proximity effects can reduce spin Hall conductivities [29]. Furthermore, spin pumping does not suffer from the conductance mismatch problem that hinders effective electrical spin injection into low conductivity materials [60]. For example, spin current injection via spin pumping has been demonstrated into semiconductors, such as Si [61] and GaAs [62], organic semiconductors [63], and even two-dimensional systems, such as graphene [64] and topological insulators [65,66]. With respect to the later, it is also interesting to note that spin pumping has been used to investigate the spin transport in two-dimensional interface states, which give rise to Rashba-type spin-orbit coupling [67,68]. Lastly, it has been recently suggested that spin pumping, can even inject spin currents into insulating antiferromagnets, such as NiO, where a spin current might be mediated by magnon excitations [69].

Since spin Hall effects benefit from strong spin-orbit coupling, the materials of interest generally include heavy elements. Another effect, which has gained interest recently, also occurs at the interfaces between ferromagnetic layers with these heavy element materials; namely a chiral Dzyaloshinskii-Moriya interaction [70,71] stabilized by the breaking of inversion symmetry. An interesting consequence of this interaction is that it can stabilize chiral magnetic domain configurations [72], and favor Neél domain walls with a fixed chirality rather than Bloch domain walls in ultrathin films with perpendicular anisotropy [73–78]. It was recently observed that this stabilization of Neél domain walls with well-defined chirality in combination with spin transfer torques from spin Hall effects results in very efficient domain wall motion with electric currents [75,76]. One consequence is that

domain walls from up-to-down and down-to-up domains are affected differently by external magnetic fields within the plane of the ferromagnetic layer and perpendicular to the domain wall, as shown in Fig. 3. Figure 3(b) shows the domain wall velocity in a stack of (3 nm) Pt / (0.6 nm) $Co_{80}Fe_{20}$ / (1.8 nm) MgO patterned into 500-nm wide wires as a function of a magnetic field applied along the wire axis for an electric current density of -3×10^{11} A/m^2 [75]. As can be seen, the change of the velocity with magnetic field is opposite for the two types of possible domain walls. This is intuitively obvious, since in one case the external field is parallel to the magnetization within the domain wall, while for the other type it is antiparallel. Indeed large enough fields can reverse the direction of the magnetization in the domain wall, which then also results in a reversal of the direction of domain wall motion [76]. Remarkably the velocity of the domain wall motion due to spin Hall effect is significantly larger compared to cases where any current-induced spin-transfer torque only arises from a current traversing the domain wall. The motion can become even more efficient if the single ferromagnetic layer is replaced by two antiferromagnetically-coupled ferromagnetic layers [79]. In this case the response of the magnetization to the spin transfer torques from the spin Hall effect can result in additional exchange coupling torques, which lead to a significant increase of the domain wall velocity. From an applied point of view, the ability to manipulate domain wall motion is of interest for racetrack memories, where information is encoded in the presence or absence of magnetic domain walls, which can be reversibly shifted via the application of electric charge currents [80].

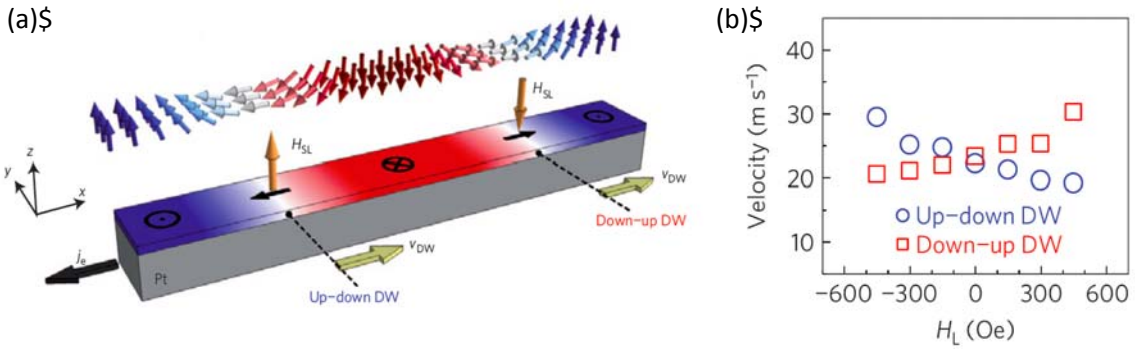

Fig. 3: (a) Schematic of chiral Neél domain walls in Pt/Co/MgO. H_{SL} indicates the effective field that is due to spin transfer torques from spin Hall effects, resulting in both type of domain walls (up-to-down and down-to-up) moving in the same direction against the direction of electron flow j_e. (b) Response of the domain wall velocity measured at constant current density j_e = -3×10^{11} A/m^2 to a magnetic field H_L applied along the direction of the wire. Adapted by permission from Macmillan Publishers Ltd: Nature Materials from [75], copyright 2013.

For thin films that are more extended than the wires discussed above, the chirality of the domain walls can give rise to more complex spin textures known as skyrmions [81–86]. Magnetic skyrmions are spin textures that were first discovered in materials with bulk chiral Dzyaloshinskii-Moriya interactions [87], where in a narrow temperature and field region the spin structure is topologically distinct from a homogenous magnetization state. Namely, tubes of magnetization are formed that are antiparallel aligned to that of the surrounding matrix (see Fig. 4), which is aligned with the external magnetic field. The name skyrmion is derived from the name of Tony Hilton Role Skyrme, who developed the concept of similar topological solitons for describing baryons, such as neutrons and protons, in

nuclear physics [88]. What makes this magnetization structure topologically distinct is the spin structure at the domain wall boundary, where the spins point into every possible three-dimensional direction [89–91]. As a result, these magnetic skyrmions are robust against perturbation and can behave like quasiparticles that can be manipulated via magnetic field gradients and charge- and heat-currents. Depending on the nature and symmetry of the chiral Dzyaloshinskii-Moriya interactions the actual spin structure of the skyrmion can be slightly different: there are vortex-like skyrmions [see Fig. 4(a)], where the intermediate spins are aligned tangentially to the circular structures (resembling a Bloch domain wall), and hedgehog-like skyrmions [see Fig. 4(b)], where the intermediate spins point along a radial direction (resembling a Néel domain wall). However, both structures are topological equivalent. With few exceptions, such as GaV_4S_8 [92], skyrmions in materials with bulk chiral Dzyaloshinskii-Moriya interactions form typically vortex-like structures, while skyrmions in magnetic multilayers with chiral Dzyaloshinskii-Moriya interactions due to interfacial symmetry breaking result in hedgehog-like structures. It should be noted that vortex-like skyrmion magnetic structures can also be stabilized in magnetic multilayers by geometric confinement in the absences of interfacial chiral Dzyaloshinskii-Moriya interactions [93,94]. Lastly, it should be noted that skyrmions are known to be stabilized at room temperature only for a few bulk materials [95], while skyrmion structures have been observed at room temperature in a variety of magnetic multilayer combinations [84–86,94].

Another important consequence of the distinct topology for skyrmionic spin structures, is that they result in emerging virtual magnetic fields giving rise to a

deflection of electric charge motion (topological Hall effects) [96,97]. This in turn also gives rise to a back-action on the magnetic skyrmions, meaning that they can be efficiently moved even with low charge currents [98]. At the same time the confined geometry of skyrmions minimizes their pinning. This was recently demonstrated in micromagnetic simulations that also explored the feasibility of using skyrmions as information carriers in magnetic wires [99], similar to earlier concepts of domain-wall racetrack memories [80].

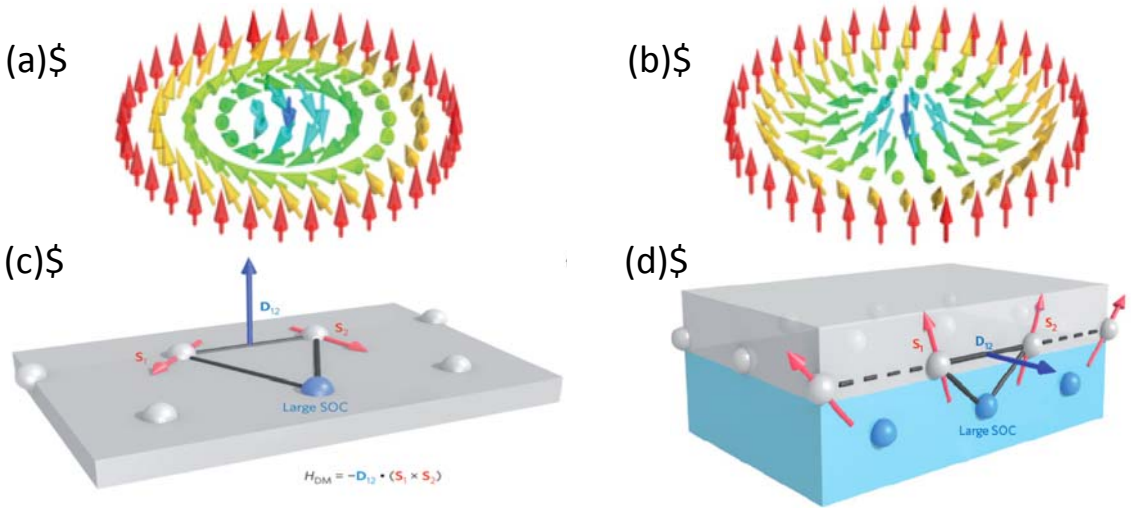

Fig. 4: Schematics of (a) a vortex-like (Bloch) and (b) a hedgehog-like (Néel) magnetic skyrmion structure. The vortex-like skyrmions are typical for skyrmions generated by bulk (c) chiral Dzyaloshinskii-Moriya interactions, such as in B20 compounds, while the hedgehog-like skyrmions are generally stabilized from interfacial (d) chiral Dzyaloshinskii-Moriya interactions. Adapted by permission from Macmillan Publishers Ltd: Nature Nanotechnology from [99], copyright 2013.

One of the key challenges to make skyrmions useful for information encoding is the ability to generate skyrmions on demand. For this one wants to operate in a

region of the magnetic phasediagram, where metastable skyrmions can coexists with the fully saturated magnetic state, so that alternatively the presence or absence of a skyrmion can persist for long time scales. An early demonstration of skyrmion generation utilized a spin-polarized scanning tunneling microscope. Using this approach at cryogenic temperatures a spin polarized current from the magnetic tunneling tip can provide sufficient torque on the magnetization enabling the creation and annihilation of metastable skyrmions in PdFe bilayers on an Ir(111) surface [82]. But it is unclear whether the skyrmions created in this system are mobile, and if this approach can be extended to room temperature. More recently it was shown that skyrmions can also be generated from instabilities [84] that are similar to Rayleigh-Plateau instabilities in surface-tension-dominated fluid flow [100]. Namely, geometrically constricting the charge current flow in a perpendicular magnetized film with chiral domain walls and strong spin Hall spin transfer torques results in an inhomogeneous effective field that drives the domain-wall motion [see Figs. 5(a)-(d)]. As a consequence the magnetic band domains expand, resulting in increased surface tension, which ultimately leads to the break up of a band domain into individual skyrmion bubbles. This is experimentally shown in Figs. 5(e) and (f), where the domain structure is imaged using the magneto-optic Kerr effect (MOKE) [101] for a Ta (5 nm) / $Co_{20}Fe_{60}B_{20}$ (1.1 nm) / TaO_x (3 nm) trilayer in a small perpendicular magnetic field of -0.5 mT. By applying a single electric current pulse for 1 s of magnitude 5×10^5 A/cm^2 (normalized by the width of the wide parts of the wire) the magnetic stripe domains on the left side of the 3-μm wide constriction are transformed into many skyrmion bubbles [84].

Measurements with smaller currents reveal the gradual generation of individual skyrmions, similar to the mechanism schematically depicted in Figs. 5(a)-(d). After generating the skyrmions with larger pulses, their motion can be investigated with smaller currents. These measurements reveal a ratio of speed-to-current density that is comparable to measurements with individual domain walls [75,76], but the critical current density is reduced by about three orders of magnitude [76] to ~10 kA/cm^2. This suggests that previous theoretical predictions about low-current manipulation of skyrmions in thin film systems are indeed viable, and that therefore the goal of using topological charge instead of electric charges for memory and/or logic devices is feasible. It should be noted that the fact that skyrmions are mobile in two dimensions, unlike domain walls in linear devices, could offer additional opportunities. In fact for magnetic-field-driven skyrmion bubbles, it already has been demonstrated that two-dimensional patterns can be moved coherently [102], which opens the way to massively parallel racetrack memories.

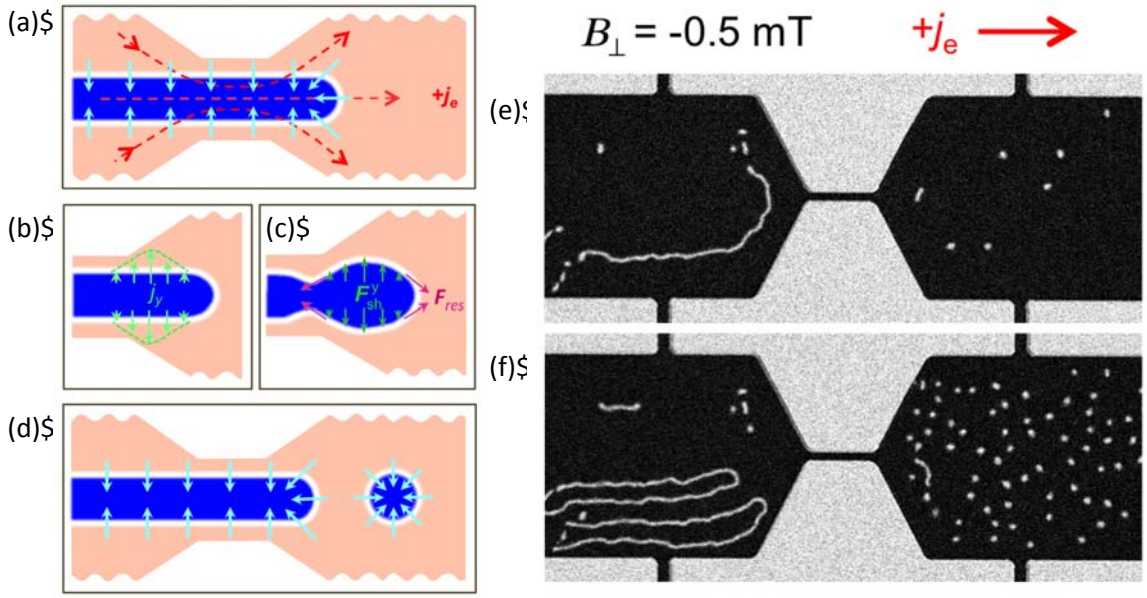

Fig. 5: (a)–(d) Schematic of skyrmion formation from stripe domains. (a) By placing the stripe domain into a constriction there is a laterally varying current distribution that gives rise to inhomogeneous spin transfer torques. (b),(c) This results in lateral forces expanding the stripe domain. (d) Ultimately the surface tension of the domain wall will lead to a bubble domain breaking off from the stripe domain. (e) Magneto-optic Kerr effect (MOKE) imaging of domain structure at $B_\perp$ = -0.5 mT before electric current is applied. The constriction is 3-μm wide and 20-μm long, while the wide parts of the wires are 60-μm wide. (f) MOKE imaging after current pulse with a density of $j_e = 5\times10^5$ A/cm^2 in the wide parts of the wire, resulting in the formation of many skyrmions. Adapted from [84]. Reprinted with permission from AAAS.

II. Spin-Caloritronics

A modern paradigm of spintronics is to investigate the interplay between charge currents and spin structures and dynamics. The spin Hall effects discussed above have been instrumental in ushering in a new field of research, spin caloritronics [103], where in addition to purely charge-current-driven effects also the interaction of spin and charge degrees of freedom with heat currents is investigated. The key phenomenon that started this field is the spin Seebeck effect [104–106]. While the original spin Seebeck measurements in a transverse geometry [104,107,108] have been controversial because of complications with analyzing the results due to other magneto-thermoelectric effects, in particular anomalous Nernst effects, [109–111], the longitudinal spin Seebeck [104,105,112–114] effect is better established. The

typical measurement geometry is shown in the inset at the top of Fig. 6(a). Here a ferromagnetic insulator, yttrium iron garnet (YIG), is capped by a thin layer of Pt, which is a material with a large spin Hall effect, and a voltage perpendicular to the magnetization direction is detected along the Pt layer upon applying a thermal gradient across this bilayer, as shown in Fig. 6. The thermal gradient can be established by contacting the sample to different temperature sinks [98,99], laser heating [115], current-induced heating [116], or integrating independent heating elements into the devices [117]. This effect is generally understood in terms of magnon heat-currents, which generate via spin pumping a diffusive spin current in the adjacent paramagnetic metal that is then converted into transverse voltages by the spin Hall effect [118–121]. Recently, also the reciprocal spin Peltier effect has been observed, where a temperature modulation dependent on the magnetization direction in YIG was observed in response to spin accumulation generated at a YIG/Pt interface from direct spin Hall effects [122]. It should be noted that beyond these novel effects that are considered to depend on heat transport via magnons, there are also effects related to thermal transport at interfaces with conductive ferromagnets, which are spin-dependent versions of ordinary Seebeck and Peltier effects due thermal transport by spin-polarized charge carriers [122,123].

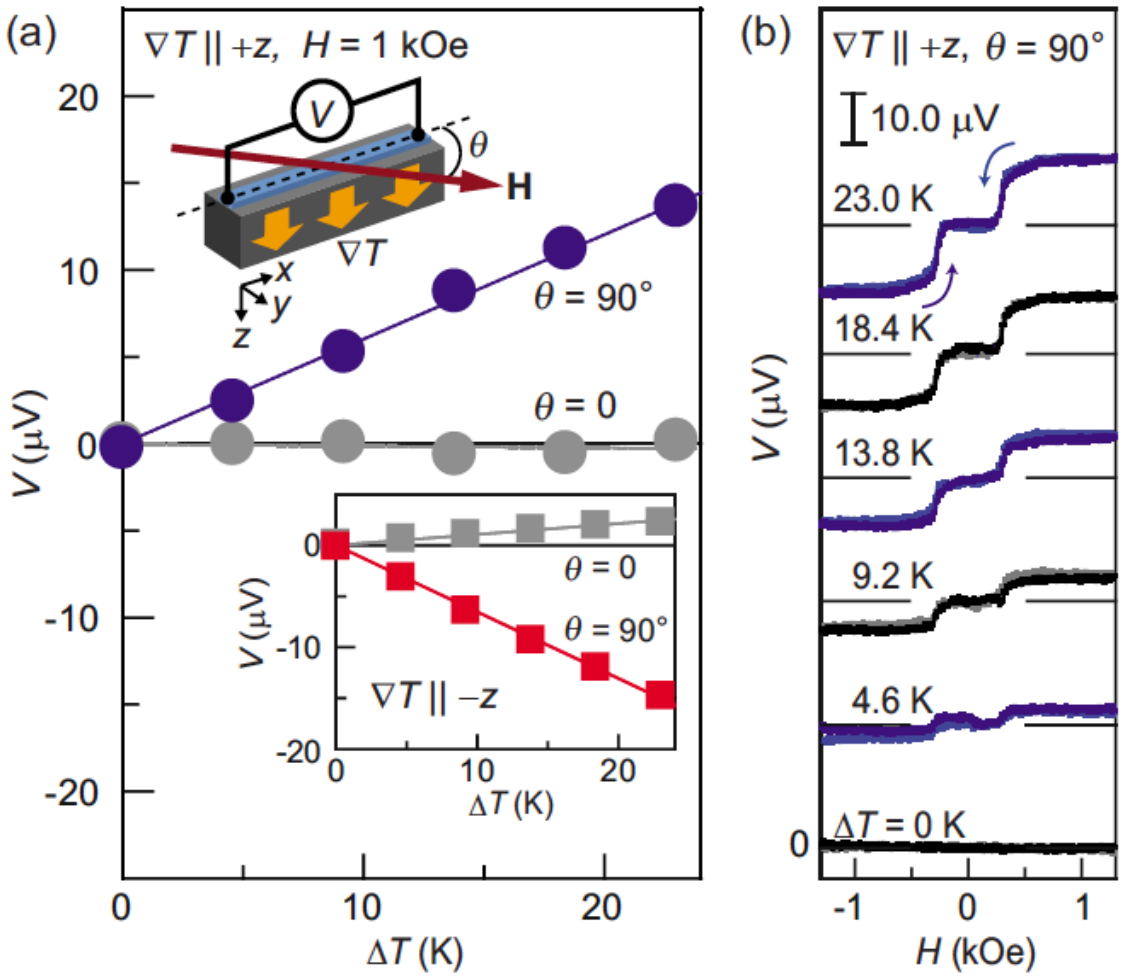

Fig. 6: (a) Longitudinal spin Seebeck voltage as a function of temperature difference across single-crystal yttrium iron garnet with a 15-nm thick Pt wire measured with a magnetic field H = 1 kOe applied along either parallel (0°) or perpendicular (90°) to the Pt wire. (b) Field dependence of the spin Seebeck voltage for the indicated temperature differences. Reprinted figure with permission from [106]. Copyright 2010 by AIP Publishing.

The realization that there are non-trivial connections between heat and spin transport has opened a variety of fundamental questions as well as new

opportunities for applications. Recently An *et al.* demonstrated the interplay between heat transport and magnons explicitly [125]. Using infrared imaging they observed that the excitation of surface magnons with non-reciprocal propagation directions results in an asymmetric temperature distribution around the microwave antenna used for the magnon excitation. This then raises the question, whether spin currents can be used for local thermal management [126]. At the same time it might be possible to use spin Seebeck effects for large-scale thermal energy harvesting [127,128], which has advantages due to the low-cost of the materials and the straightforward scaling given by the transverse nature of the voltage generation in spin Seebeck structures. On a more fundamental level, it has been suggested theoretically that magnon heat currents can give rise to spin transfer effects [129] that result in the motion of magnetic solitons, such as domain walls [130,131] and skyrmions [132]. Experimentally this has recently been demonstrated for domain wall [133] and magnetic skyrmion motion [134]. In addition the ability to generate macroscopic spin currents from temperature gradients has been used for investigating spin transport phenomena, *i.e.*, comparing spin Hall effects for different materials [135]. Lastly, the recent interest in heat currents in the context of spin current has also revived interest in well-established magneto-thermal transport phenomena, especially the anomalous Nernst effect. Towards this end the anomalous Nernst effect has been used to image domain structures [115] and for the detection of spin waves [136]. The later has been demonstrated for waveguides of permalloy ($Ni_{81}Fe_{19}$), where spin-waves are excited with a co-planar microwave antenna, see Fig. 6(a). The power dissipated by the spin waves leads to a vertical

temperature gradient [see Fig. 7(b)], which in turn gives rise to measurable Nernst voltages [see Fig. 7(c)]. Besides providing a remarkable signal-to-noise ratio, this approach for spin wave detection has the advantage that, unlike optical or inductive techniques, it is not limited by the wavelength of the spin waves. For example, the detection of spin waves down to wavelengths of 125 nm has been demonstrated, which opens the door to investigate exchange-dominated spin waves. Thus, ideas inspired by the exploration of spin caloric effects may impact investigations beyond simply understanding the interplay of spins and heat.

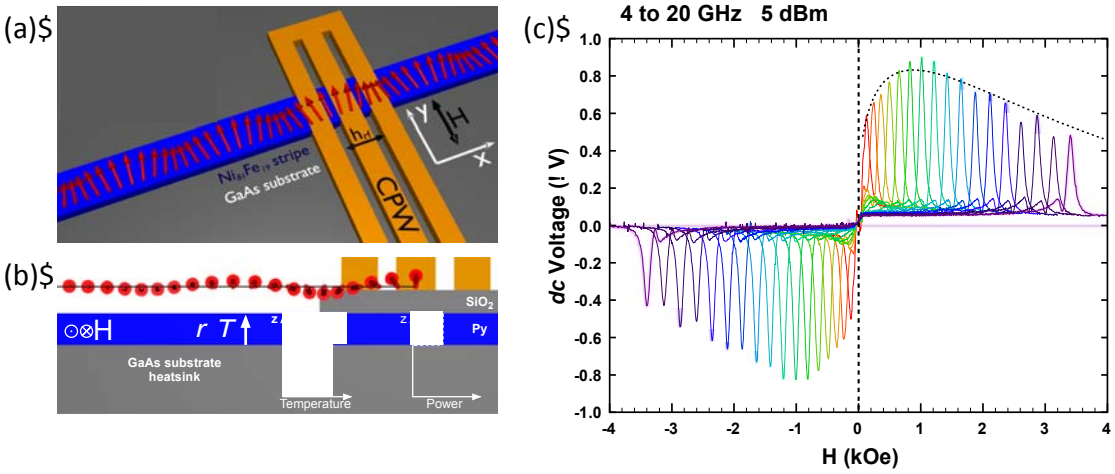

Fig. 7: (a) Schematic of a spin-wave waveguide fabricated from permalloy with a coplanar waveguide for spin-wave excitation. (b) The energy absorption and dissipation by the spin waves is confined to the permalloy layer, but due to the GaAs substrate acting as a heat sink, this creates a temperature gradient across the thickness of the permalloy layer. (c) Resultant Nernst voltage as a function of applied field for various excitation frequencies from 4 to 20 GHz. The dotted line indicates a theoretical estimate for the dissipated power by the spin waves.

Reprinted figure with permission from [136]. Copyright 2012 by the American Physical Society.

III. Magnonics

As discussed in the previous section, spin waves can play an important role for the connection between heat and diffusive spin currents. Spin waves are the fundamental quasiparticle excitations of magnetically ordered systems and hence are also referred to as magnons. Like diffusive spin currents, spin waves are associated with angular momentum transfer, but in contrast to diffusive spin currents they do not require the actual motion of spins in real space. The interaction between spins, both close-range exchange coupling, as well as long-range dipolar coupling, establish the coherent spin dynamics. At the same time the dissipation of spin waves can be low in insulating magnetically ordered systems [137], which can result in spin waves propagating over much larger distances than diffusive spin currents. As a consequence, spin waves have been envisioned as information carriers for low-power data storage and processing, which is now known as the field of magnonics [138–140]. Besides the advantage of low power dissipation, spin waves also offer the opportunity to harness their coherence and thus encode information both in their amplitude and phase. For this it is important to note that their frequencies (GHz to THz) and wavelengths (which can be as small as a few nm) are well matched to today's technological requirements for information technologies. The coherent properties of spin waves have already been exploited for a first implementation of logic gates based on the interference of two

spin-wave signals with control of their relative phase [141]. In addition, new spin-wave excitation schemes based on spin-transfer torques may enable the controlled generation of short wavelength spin waves along well-defined propagation directions [142].

Furthermore, the propagation of spin waves can be locally controlled via tailoring of magnetic properties [143] and/or by application of magnetic fields [144,145]. This idea is demonstrated by introducing the concept of a spin-wave multiplexer, as shown in Fig. 8. Using local Oersted fields through an adjacent conducting layer enables the selective rotation of the magnetization in a permalloy wire perpendicular to the wire direction. In contrast the non-current carrying sections of the device will have the magnetization aligned with the wire direction due to shape anisotropy. Since the frequency for spin waves propagating perpendicular or parallel to the magnetization is significantly different, this results in the spin waves being confined to paths that can be selected by controlling the direction of the charge flow.

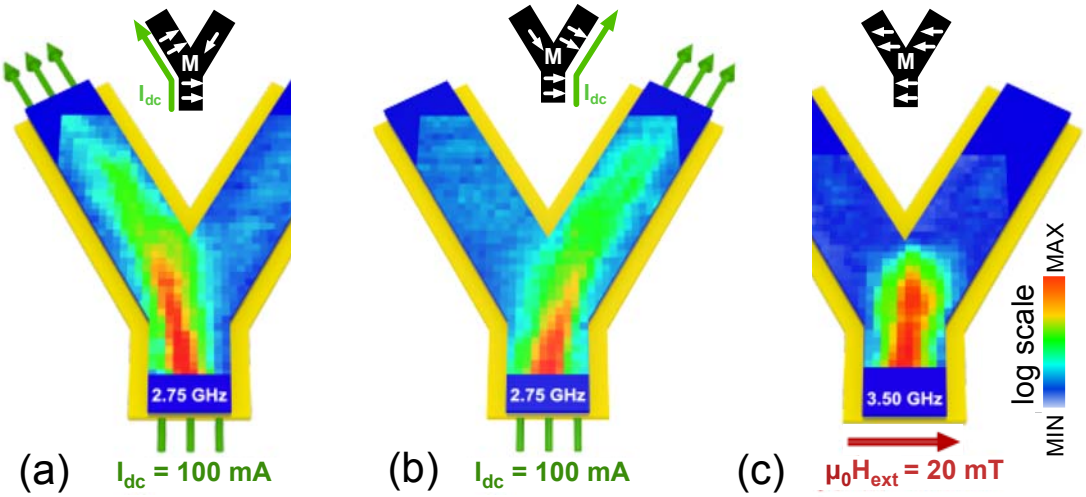

Fig. 8: Demonstration of a spin-wave multiplexer. Spatially-resolved Brillouin light scattering is used to image the spatial distribution of the spin waves, which are excited at the bottom of a Y-shaped permalloy waveguide (30-nm thick, 2-μm wide) by a local microwave antenna. Local Oersted magnetic fields generated via charge currents through a separate 50-nm thick conducting Au layer underneath the permalloy wave guide enables the spin waves to be selectively steered to the left (a) or to the right (b). (c) With the charge currents replaced by a uniform external magnetic field the spin waves terminate at the junction. Adapted by permission from Macmillan Publishers Ltd: Nature Communications from [145], copyright 2014.

The other attractive feature of spin waves is that the inherent non-linearity of magnetization dynamics provides novel pathways for manipulation due to multi-magnon scattering processes. Based on this idea, a magnon transistor, where magnon propagation could be controlled by four-magnon scattering processes was recently implemented with a modulation of the transmitted magnon amplitude by three orders of magnitude [146]. Furthermore, four-magnon scattering conserves the overall magnon number, and, therefore, upon sufficiently high pumping the scattering may thermalize the magnons and result in the formation of a Bose-Einstein condensate. Experimentally this is observed even at room temperature by exciting magnons via parametric pumping [147]. This provides exciting opportunities to develop devices that take full advantage of the coherency of the

magnon condensate [148] and to explore phenomena in analogy to superconducting devices, such as spin supercurrents [149–152] and Josephson effects [153].

Since the dispersion of spin waves in thin films is strongly influenced by dipolar interactions, which give rise to demagnetizing fields, it follows that the properties of spin waves can be tuned by the changing the geometry via patterning. In particular, periodic structures can be used to define magnonic crystals [138,154,155], where the propagation of spin waves is controlled by allowed and forbidden frequency bands. Even topologically non-trivial magnonic band structures generated by periodic patterning are conceivable that give rise to chiral edge modes [156,157].

Besides patterning magnetic films to manipulate their magnetization dynamics, another opportunity is given by the fact that magnetic systems can often support a wide variety of remanent magnetic states. A particularly interesting case is given by magnetic vortex singularities that form in soft-magnetic disks [158]. Here the geometric confinement results in a magnetization that swirls in-plane clockwise or counterclockwise and forms a nano-size vortex core, where the magnetization points out-of-plane (up or down). This vortex core has distinct gyrotropic dynamics, where the direction of dynamic motion is determined by the polarity of the magnetization in the core [159–161]. While the dynamics is degenerate for isolated disks, interactions between disks can lift the degeneracy [162]. In fact for pairs of interacting vortices it was observed that the frequency of the dynamics depends on whether the core polarities were parallel or anti-parallel [163]. This idea can be generalized to a large two-dimensional vortex array forming a

reprogrammable magnonic crystal, where the band structure of the spin waves is determined by the configuration of individual vortex cores [164].

A crucial aspect of realizing a truly reprogrammable magnonic crystal is the ability to control the magnetization states, which give rise to different dynamic resonances. Towards this end, an elegant approach akin to spectral hole burning [165] was recently realized. This is shown in Fig. 9, where absorption spectra of the gyrotropic motion of two overlapping permalloy disks (48-nm thick, 1-μm diameter each) have been measured. In this case the direct contact gives rise to strong interactions between the two disks. As can be seen in Fig. 9(c) there is a distinct difference in the gyrotropic motion of the vortex cores depending on whether the polarization of the cores are parallel or antiparallel relative to each other. This spectrum was obtained from >1,000 disk pairs with a microwave power of -10 dBm in the as-grown state, where the relative core polarizations are random. Upon applying microwaves with 10-dBm power at either of the two absorption peaks in Fig. 9(c) the spectrum changes to only a single absorption peak. This indicates that all double-disk pairs switched to the same relative core-polarization state, which is opposite to the state that corresponds to the frequency where the excitation occurred. In other words, the high power excitation leads to switching to the non-resonant ground state, which does not respond to the excitation. The same idea can be generalized to more extended arrays of coupled vortices [166] and it has been shown that the switching between different remanent magnetization states can be achieved at sub-microsecond time scales [167].

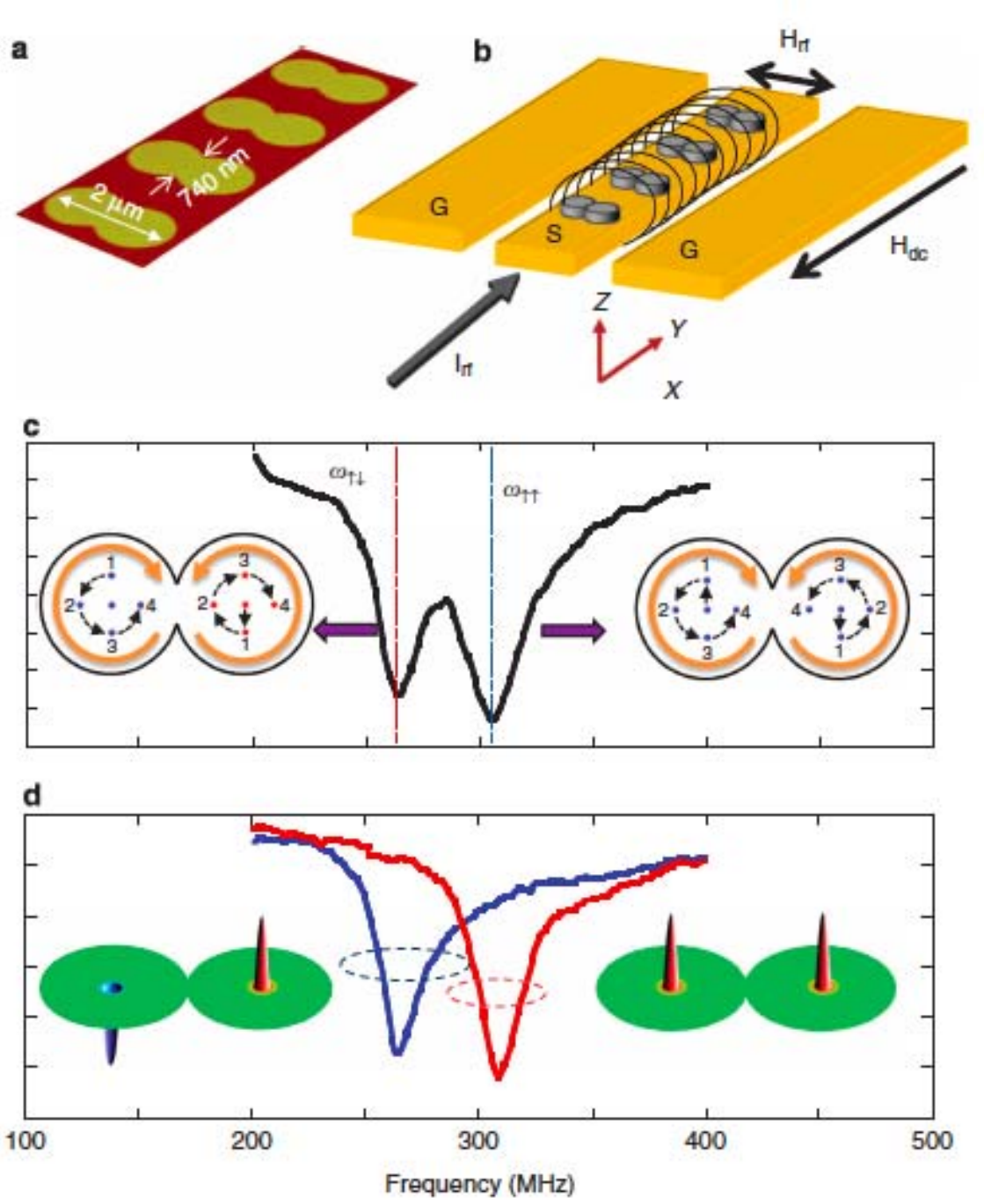

Fig. 9: (a) Atomic force microscopy image of structures consisting of two connected disks, each 1 μm in diameter. (b) Schematic of the double-disk structures integrated with a co-planar waveguide for inductive microwave absorption spectroscopy. (c) Absorption spectrum at remanence for an array of double-disk structures with

random relative orientation of vortex core polarizations. The insert indicates the relative chiralities of the corresponding gyrotropic motions. (d) Absorption spectra measured after high *rf*-amplitude excitation at either $\omega_{\uparrow\downarrow}$ or $\omega_{\uparrow\uparrow}$ as indicated in (c). The inset shows the corresponding global relative core polarizations. Adapted by permission from Macmillan Publishers Ltd: Nature Communications from [172], copyright 2012.

Interestingly, the idea that different remanent states may lead to distinct magnetization-dynamics signatures is not limited to coupled vortices with different core polarization. Micromagnetic simulations of artificial spin ice structures, which can include topological monopole defects, show distinct dynamic features correlated with the presence of these topological defects [168]. Thus, it is conceivable that in these systems resonant excitations may lead to a reorganization of the magnetic structure, which in turn modifies the dynamic response. Since this suggests that complex responses are dependent on the history of the dynamic inputs, this may open novel pathways for neuromorphic computation [169], where information processing is based on adaptive processing of analog information and thereby resembling the functionality of the natural brain. Furthermore, this is the underlying principle for magnetic quantum cellular automata [170], which may be scaled down to the single-atom level [171]. Thus, many potential avenues are available to extend these intriguing ideas.

IV. Ultrafast spin-photonics

For the past fifteen years the term nano has been used to describe a dominant theme in materials research. What theme or themes might dominant in the coming fifteen years? While it is always quite difficult to predict the future, it is likely that ultrafast phenomena will play an important role. This is both because of developments in laser technology that permit bench-top experiments in the femtosecond realm, as well as developments in fourth-generation light sources the deliver short x-ray pulses by means of free electron lasers (FEL) that utilize linear accelerator sources. An added value is that both bench-top and FEL sources deliver coherent light.

One might ask what is the shortest timescale that makes physical sense in the world of materials. We know that timescales of the order of 10^{-43} s (1 Planck time) are relevant in discussing the earliest evolution of the universe within the big-bang theory. But in the universe that we live in presently, the time it takes light to traverse the distance of an atom $\sim 10^{-18}$ s (an attosecond), or of an atomic nucleus, $\sim 10^{-21}$ s, a zeptosecond, is about as short as imagination can take us. Today's fast lasers typically deliver pulses in the sub-picosecond range of $\sim 10^{-13}$ to 10^{-14} s (tens of femtosecond range; a record of 67 attoseconds was set in 2012 [173]). Thus, we are not at the ultimate limit of time, but such pulses are fast enough compared to most chemical and physical processes of interest to enable observing them in stopped action in pump-probe experiments.

Hence, condensed matter physicists can imagine witnessing events such as the birth of elementary excitations. This certainly represents a new realm for exploration. New questions emerge, such as: does the physics we know apply to

ultrafast events? A problem is that the energy density of short pulses of light can be such that the pulsing blows apart the object meant to be observed [174]. Thus, the observation time is limited because the object will soon not exist. Certainly challenges abound here that readily could span a fifteen-year research agenda.

Within the realm of ultrafast spin-photonics, new and engaging magnetization dynamics phenomena have already been reported that signal fruitful paths to explore. We will visit a few of these in order to give a sense of the richness of the field. Necessarily we combine ultrafast with ultra-small because there is obvious technological interest in the physics of magnetic switching. Today's magnetic bits respond on the nanosecond timescale, but new evidence points to possibilities that are a thousand times faster via spin-photonic interactions. Whenever a technology can be accelerated by three orders of magnitude, we are outside the realm of incremental advances and possibly entering the realm of revolutionary advances. Thus, there is the excitement that information technology can continue along its path of development. Of course this also requires overcoming today's thermal limitations, but this is already on the agenda to address by means of basic and applied research.

There are many publications on short timescale magnetic phenomena. Some representative experimental pump-probe papers with useful reference lists include spin-resolved photoemission experiments [175], angle-resolved photoemission experiments [176], Faraday effect studies [177], and Kerr effect studies [178–181]. While these experimental papers also tend to contain mechanistic and theoretical discussions, there are also representative theory papers by Oppeneer and Liebsch

[182] and by Carva, Battiato and Oppeneer [183].

The papers by Beaurepaire, *et al.* [184] and Siegmann *et al.* [185] were instrumental in launching the field. Beaurepaire, *et al.* [184] utilized pump-probe, ultra-fast magneto-optics to show that the spin system of ferromagnetic nickel responded on the ps timescale, much faster than the lattice can respond. Siegmann *et al.* [185] also utilized magneto-optics, but in a static mode to characterize what happened to CoPt alloy films after being subjected to the huge transient magnetic field created by an ultrafast 50-GeV electron pulse, provided by the Stanford linear accelerator (SLAC), shot through the film. Siegmann's team [186] subsequently refined their work utilizing Co/Pt multilayers. The late Hans-Christoph Siegmann is regarded as the father of spin-polarized electron spectroscopies. He could also be considered a father of ultrafast magnetization phenomena. There is an excellent reference book by Stöhr, and Siegmann [187]. There are also two excellent reviews of ultrafast magnetization phenomena by the Nijmegen group of Kirilyuk, Kimel and Rasing [188,189]. Below the role of the Nijmegen group is discussed in advancing the field into a new realm.

Recently great interest has been generated by experiments on optical control of magnetic switching at ultrafast speeds. These are on compounds of rare earth – transition metal ferrimagnetic films performed by the Nijmegen group and their collaborators. They found that circularly polarized ultrafast laser pulses are able to switch the magnetization state of the film. This inspired a host of possible theoretical explanations. One involves an inverse Faraday effect. In the Faraday effect linearly polarized light rotates on transmission through a magnetized

medium. Since the films under consideration are not transparent, as are typical Faraday glasses, rather than the light being transmitted, it is partially absorbed and partially back reflected, as in the Kerr effect. This can be viewed as a double Faraday effect (one on the way into the medium and the other on the way back out). Thus, the reflected light that emerges from the medium becomes elliptical (or takes on some circularly polarized character). This is because linearly polarized light can be decomposed into two equal, complementary (left and right) circularly polarized components. Within the magnetized medium these two components behave (reflect and absorb) differently. Thus there is an imbalance in the two recombined components on exiting the medium. This leads to the light acquiring some circular (elliptical) character. In the inverse effect the circularly (or elliptically) polarized light changes the magnetization of the medium it passes through. If the effect is large enough, it can even switch the magnetization state. Qualitatively, this is what was observed experimentally, a switching of the magnetization state.

It is also known that the spin relaxation times for rare earths and transition metals are different because the *f*-electron spins of the rare earth are more isolated (localized) than the *d*-electron spins of the transition metal. Thus, an *f*-electron spin system could take longer to equilibrate after laser pulse excitation (that can raise the spin system to temperatures that are above characteristic magnetic ordering temperatures). This can lead to non-equilibrium transient states of the ferrimagnetic system where the two magnetic sublattices have parallel (rather than antiparallel) magnetization. Such a transient state can control interesting switching dynamics on cooling, especially since such films might traverse a compensation

point on cooling back to their equilibrium temperature. At high spin temperatures the magnetization of the transition metal dominates, while below the compensation point the magnetization of the rare earth is larger, causing it to dominate (meaning that it aligns with, not against, an externally applied magnetic field). An example is shown in Fig. 10 taken from Radu *et al.* who utilized x-ray magnetic circular dichroism (XMCD) to follow the magnetization dynamics of the Fe and Gd [190]. Their sample was an amorphous ferrimagnetic alloy film of GdFeCo at 83 K. They estimated that the spin temperature rose to ~1,500 K due to the laser excitation, while the compensation temperature is only 250 K. The paper [190] also presents a model that quantitatively describes the experiment for which the Fe relaxes more rapidly from the laser pulse than the Gd. A follow-up study by Ostler *et al.* [191] showed that experiments and modeling of ultrafast magnetization switching dynamics agreed again in configurations where the GdFeCo were initially above the compensation temperature and the laser pulsing raised the spin temperature above the Curie temperature in the absence of an external magnetic field. This again represents a striking result.

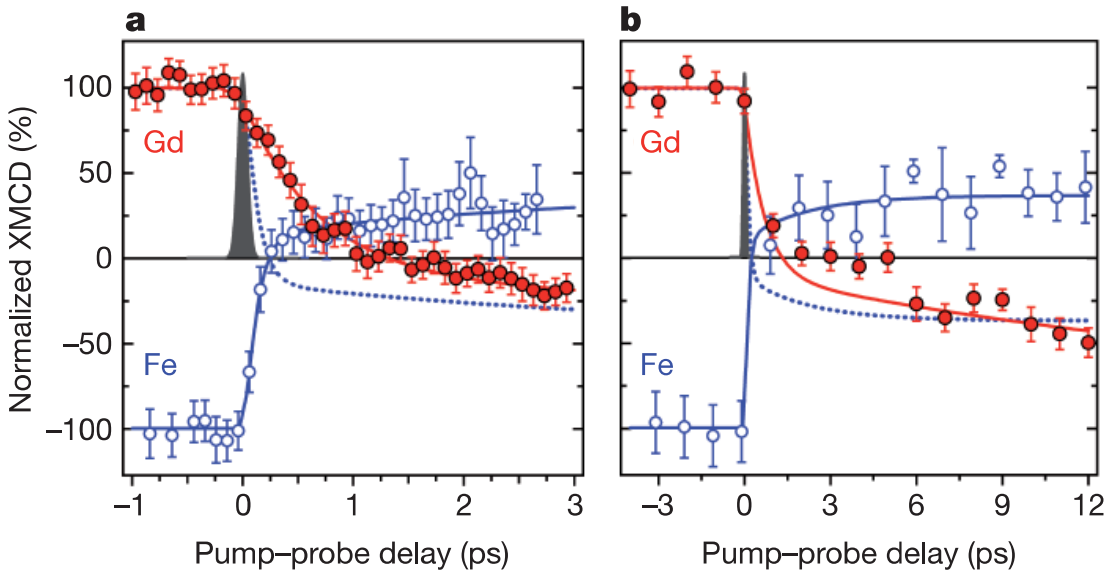

Fig. 10: XMCD data taken from the work of Radu *et al.* [190] that shows the Gd and Fe magnetic moment responses in GdFeCo due to 60-fs laser excitation on 3-ps (a) and 12-ps (b) timescales. The Gaussian in (a) illustrates the 0.1-ps experimental time resolution. The solid lines are fits to the data, as described in Ref. 175, and the dashed lines represent the opposite sign of the Fe fits.

There had been additional ideas proposed earlier that could potentially provide insight into such phenomena. One involves the transfer of angular momentum from the circularly polarized pulse to the spin system of the medium, another invokes the action of spin currents induced by the laser. These ideas are outlined and referenced in the recent work of Mangin *et al*. [192] They are intriguing in that they deepen our understanding of the interaction of light and matter on ultra-short time scales. They also suggest further experimentation to sharpen our insights into the fundamental processes of interest.

This is precisely what happened. The field was subsequently opened further by a set of fast pulse laser experiments performed by an international collaboration of Mangin *et al.* [192] followed by that of Lambert *et al.* [193] The work of Mangin *et al.* demonstrated that the range of materials that could be optically switched via ultrafast pulses was broader than just amorphous rare-earth-transition metal ferrimagnetic alloys, but included synthetic ferrimagnetic multilayer films that are crystalline and that could be rare-earth free. The follow-up work by Lambert *et al.* further generalized the materials systems that could be optically switched to include *ferromagnetic* systems, not just ferrimagetic ones. These studies were performed on multilayer films including $3d/5d$ transition metal multilayers, such as Co/Pt with perpendicular magnetic easy axes, and even on simple thin metallic films. The laser pulses in both of these studies included linearly polarized light (that possess no net angular momentum) as well as left and right circularly polarized light.

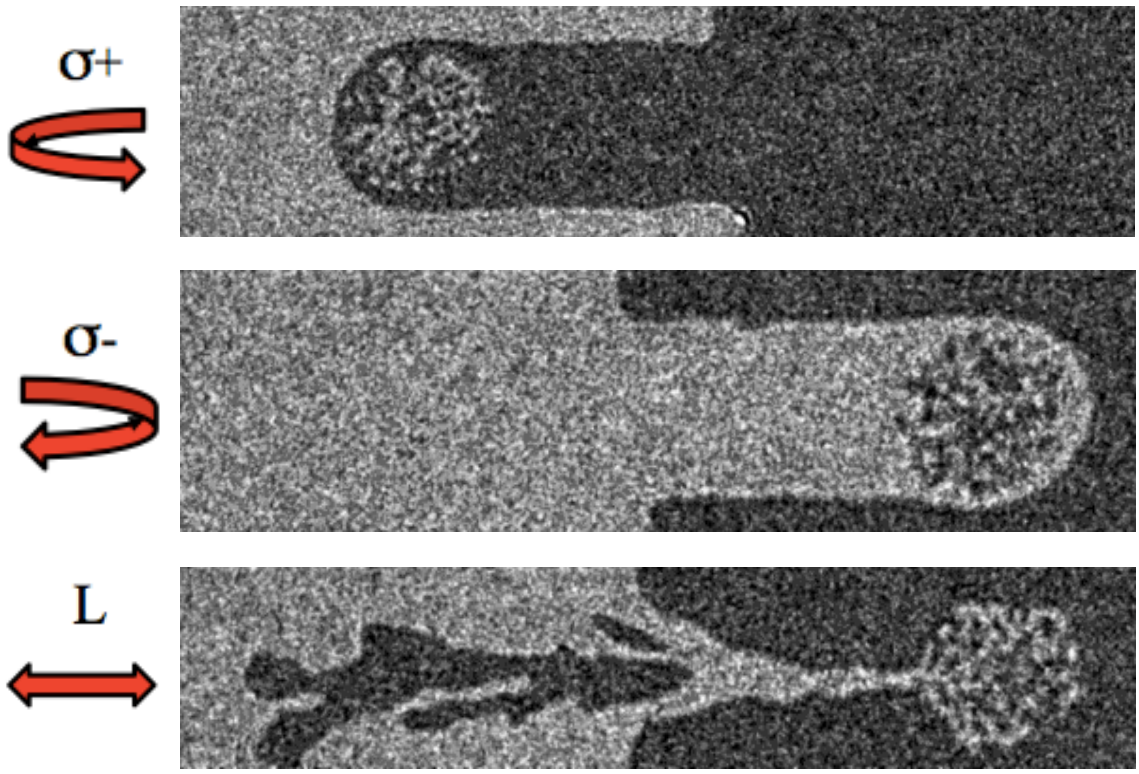

Fig. 11: Faraday microscopy images for a $[Co(0.4\ nm)/Pt(0.7\ nm)]_3$ film sample taken subsequent to sweeping across each image a ~0.1-ps laser pulse of 800-nm (1.55 eV) wavelength with a repetition rate of 100 kHz without any applied magnetic field. The light/dark contrast represents the perpendicularly oriented magnetic domains of opposite orientation. The sample originally had a domain wall midway across it vertically. Scanning the laser horizontally across each image changed the contrast from light-to-dark or dark-to-light, thus switching the magnetization. There is also fine structure in the switched domains, especially in the bottom image, as discussed by Lambert *et al.* [193] The process appears to be statistical since multiple pulses seem to be needed for the switching. The figure is adapted from the supplemental material of Ref. 193. Reprinted with permission of AAAS.

This is shown in Fig. 11 for a $[Co(0.4\ nm)/Pt(0.7\ nm)]_3$ sample. The images in the figure were taken by means of a Faraday microscope subsequent to the sample being pulsed with a ~0.1-ps laser beam. The figure shows the three polarization directions schematically to the left. The region imaged originally had a magnetic domain wall, which separates two perpendicularly oriented domains, that ran vertically through the middle, as indicated by the dark/light contrast. The laser beam was swept horizontally across the domain wall. The length scale is ~0.1 mm across each image. The work demonstrates all-helicity optical switching of the magnetization of a ferromagnetic film. It also shows magnetic-domain fine structure, especially in the bottom image that is associated with the linearly polarized light pulse, as discussed in Lambert *et al.* However, there are two major open issues associated with this work. One is that while the paper *assumes* that the role of the helicity of the pulse persists only on the ps timescale, it does not track this time dependence in order to confirm the ultrafast nature of the switching. The Faraday images were taken subsequent to the pulsing. The other is that the mechanism of the switching still requires a theoretical understanding of its underlying mechanism. Thus, the work will undoubtedly stimulate follow-up studies in the future both experimentally and theoretically.

Despite the open issues, the striking result is that many types of films can have their magnetization switched optically, thus, ultrafast-pulse-initiated optical switching appears to be a general phenomenon. This can be likened to the early days of giant magneto-resistance (GMR), when Parkin [194] showed that GMR was a

quite general materials phenomenon, not limited to the Fe/Cr system that the Grünberg [2] and Fert [1] teams had discovered. Thus, the problem of optical switching has become even more interesting, firstly because the phenomena identified by the Nijmegen group and collaborators seems to be even more general than just applying to ferrimagnets, and secondly, because systems such as Co/Pt are already of interest to the magnetic recording community. Thus, there might be new ways to significantly speed up magnetization switching in materials that are commercially relevant to the information technology community.

V. Summary and Conclusions

This short review was meant to walk the reader through some of the interesting recent developments in the field of spintronics as viewed through the eyes of the authors. The goal was to stimulate interest in the great variety of directions the field is taking. This is a healthy sign for a maturing field. The topics of spin-orbit physics, spin-calorics, induced spin-wave effects, and ultrafast magnetization dynamics were highlighted with examples. While each of these areas is rich in basic physics, the point was also to suggest the applied aspects and opportunities for further research. Hence provocative subtitles were used, such as spin-orbitronics and magnonics. Will these ideas enter the commercial arena advancing the field of information technology? This question is of particular interest to ponder given that the present year, 2015, represents the fiftieth anniversary of the famous prediction by Gordon Moore, known as "Moore's law" [195]. Moore extrapolated into the future the rise in the packing density of transistors on a chip. Moore's visionary

prediction has since been loosely generalized to cover additional advances in the realm of information technology encompassing the mantra: *smaller, faster, cheaper, cooler*. However, the miniaturization of today's silicon technology is leading to thermal problems. This is where fields like spintronics can help, because they can involve less heat dissipation. Thus, we can envision the possibility that spintronics can provide *small* and *cool* information processing and storage systems in the future. We also see that the *fast* part is looking promising within the spintronics realm. Since economics tends to dominate the marketplace, it remains to be seen if and which emerging ideas will ultimately be *cost-effective to* manufacture. The playing field is wide open to explore!

Acknowledgement

This work was supported by the U. S. Department of Energy, Office of Science, Basic Energy Sciences, Materials Science and Engineering Division. We thank our many colleagues with whom we had discussions and fruitful collaborations. We are also grateful for the assistance of Suzanne Kokosz with the preparation of this manuscript.

References

1. M. N. Baibich, J. M. Broto, A. Fert, F. N. van Dau, F. Petroff, P. Etienne, G. Creuzet, A. Friedrich, and J. Chazelas, Giant Magnetoresistance of (001)Fe/(001)Cr Magnetic Superlattices, Phys. Rev. Lett. **61**, 2472 (1988).
2. G. Binasch, P. Grünberg, F. Saurenbach, and W. Zinn, Enhanced magnetoresistance in layered magnetic structures with antiferromagnetic interlayer exchange, Phys. Rev. B **39**, 4828 (1989).
3. I. Žutić, J. Fabian, and S. Das Sarma, Spintronics: Fundamentals and applications, Rev. Mod. Phys. **76**, 323 (2004).
4. S. D. Bader and S. S. P. Parkin, Spintronics, Annu. Rev. Cond. Matter Phys. **1**, 71 (2010).
5. M. Hilbert and O. López, The World's Technological Capacity to Store, Communicate, and Compute Information, Science **332**, 60 (2011).
6. E. Pop, S. Sinha, and K. E. Goodson, Heat Generation and Transport in Nanometer-Scale Transistors, Proc. IEEE **94**, 1587 (2006).
7. D. Weller, A. Moser, L. Folks, M. E. Best, W. Lee, M. F. Toney, M. Schwickert, J.-U. Thiele, and M. F. Doerner, High K_u materials approach to 100 Gbits/in^2, IEEE Trans. Magn. **36**, 10 (2000).
8. B. Lambson, D. Carlton, and J. Bokor, Exploring the Thermodynamic Limits of Computation in Integrated Systems: Magnetic Memory, Nanomagnetic Logic, and the Landauer Limit, Phys. Rev. Lett. **107**, 010604 (2011).
9. M. Ellis, Gadgets and Gigawatts: Policies for Energy Efficient Electronics (OECD/IEA, Paris, 2009)

10. A. Hoffmann and H. Schultheiß, Mesoscale magnetism, Curr. Opin. Solid State Mater. Sci. **19**, 253 (2015).

11. R. L. Stamps, S. Breitkreuz, J. Åkerman, A. V. Chumak, Y. Otani, G. E. W. Bauer, J.-U. Thiele, M. Bowen, S. A. Majetich, M. Kläui, I. L. Prejbeanu, B. Dieny, N. M. Dempsey, and B. Hillebrands, The 2014 Magnetism Roadmap, J. Phys. D: Appl. Phys. **47**, 333001 (2014).

12. J. E. Hirsch, Spin Hall effect, Phys. Rev. Lett. **83**, 1834 (1999).

13. A Hoffmann, Spin Hall Effects in Metals, IEEE Trans. Magn. **49**, 5172 (2013).

14. M. I. D'yakonov and V. I. Perel', Possibility of orienting electron spins with current, Sov. Phys. JETP Lett. **13**, 467 (1971).

15. M. I. Katsnelson, V. Yu. Irkhin, L. Chioncel, A. I. Lichtenstein, and R. A. de Groot, Half-metallic ferromagnets: From band structure to many-body effects, Rev. Mod. Phys. **80**, 315 (2008).

16. W. H. Butler, X.-G. Zhang, T. C. Schulthess, and J. M. MacLaren, Spin-dependent tunneling conductance of Fe/MgO/Fe sandwiches, Phys. Rev. B **63**, 054416 (2001).

17. S. Yuasa, T. Nagahama, A. Fukushima, Y. Suzuki, and K. Ando, Giant room-temperature magnetoresistance in single-crystal Fe/MgO/Fe magnetic tunnel junctions, Nat. Mater. **3**, 868 (2004).

18. S. S. P. Parkin, C. Kaiser, A. Panchula, P. M. Rice, B. Hughes, M. Samant, and S.-H. Yang, Giant tunnelling magnetoresistance at room temperature with MgO (100) tunnel barriers, Nat. Mater. **3**, 862 (2004).

19. K. Ando, S. Takahashi, K. Harii, K. Sasage, J. Ieda, S. Maekawa, and E. Saitoh, Electric Manipulation of Spin Relaxation Using the Spin Hall Effect, Phys. Rev. Lett. **101**, 036601 (2008).

20. L. Liu, C.-F. Pai, Y. Li, H. W. Tseng, D. C. Ralph, and R. A. Buhrman, Spin-Torque Switching with the Giant Spin Hall Effect of Tantalum**,** Science **336**, 555 (2012).

21. C.-F. Pai, L. Liu, H. W. Tseng, D. C. Ralph, and R. A. Buhrman, Spin transfer torque devices utilizing the giant spin Hall effect of tungsten, Appl. Phys. Lett. **101**, 122404 (2012).

22. W. Zhang, V. Vlaminck, J. E. Pearson, R. Divan, S. D. Bader, and A. Hoffmann, Determination of the Pt spin diffusion length by spin-pumping and spin Hall effect, Appl. Phys. Lett. **103**, 242414 (2013).

23. M. Althammer, S. Meyer, H. Nakayama, M. Schreier, S. Altmannshofer, M. Weiler, H. Huebl, S. Geprägs, M. Opel, R. Gross, D. Meier, C. Klewe, T. Kuschel, J.-M. Schmalhorst, G. Reiss, L. Shen, A. Gupta, Y.-T. Chen, G. E. W. Bauer, E. Saitoh, and S. T. B. Goennenwein, Quantitative study of the spin Hall magnetoresistance in ferromagnetic insulator/normal metal hybrids, Phys. Rev. B **87**, 224401 (2013).

24. J. Sinova, S. O. Valenzuela, J. Wunderlich, C. H. Back, and T. Jungwirth, Spin Hall effect, arXiv:1411.3249.

25. B. F. Miao, S. Y. Huang, D. Qu, and C. L. Chien, Inverse spin Hall effect in a ferromagnetic metal, Phys. Rev. Lett. **111**, 066602 (2013).

26. H. Wang, C. Du, P. C. Hammel, and F. Yang, Spin current and inverse spin Hall effect in ferromagnetic metals probed by $Y_3Fe_5O_{12}$-based spin pumping, Appl. Phys. Lett. **104**, 202405 (2014).

27. T. Taniguchi, J. Grollier, M. D. Stiles, Spin-transfer rorques generated by the anomalous Hall effect and anisotropic magnetoresistance, Phys. Rev. Appl.**3**, 044001 (2015).

28. W. Zhang, M. B. Jungfleisch, W. Jiang, J. E. Pearson, A. Hoffmann, F. Freimuth, and Y. Mokrousov, Spin Hall Effects in Metallic Antiferromagnets, Phys. Rev. Lett. **113**, 196602 (2014).

29. W. Zhang, M. B. Jungfleisch, W. Jiang, Y. Liu, J. E. Pearson, S. G. E. te Velthuis, A. Hoffmann, F. Freimuth, and Y. Mokrousov, Reduced spin-Hall effects from magnetic proximity, Phys. Rev B **91**, 115316 (2015).

30. Y. Kajiwara, K. Harii, S. Takahashi, J. Ohe, K. Uchida, M. Miziguchi, H. Umezawa, H. Kawai, K. Ando, K. Takanashi, S. Maekawa, and E. Saitoh, Transmission of electrical signals by spin-wave interconversion in a magnetic insulator, Nature **464**, 262 (2010).

31. Z. Wang, Y. Sun, M. Wu, V. Tiberkevich, and A. Slavin, Control of spin waves in a thin film ferromagnetic insulator through interfacial spin scattering, Phys. Rev. Lett. **107**, 146602 (2011).

32. E. Padrón-Hernández, A. Azevedo, and S. M. Rezende, Amplification of spin waves in yttrium iron garnet films through the spin Hall effect, Appl. Phys. Lett. **99**, 192511 (2011).

33. Z. Wang, Y. Sun, Y.-Y. Song, M. Wu, H. Schultheiß, J. E. Pearson, and A. Hoffmann, Electric control of magnetization relaxation in thin film magnetic insulators, Appl. Phys. Lett. **99**, 162511 (2011).

34. A. Hamadeh, O. d'Allivy Kelly, C. Hahn, H. Meley, R. Bernard, A. H. Molpeceres, V. V. Naletov, M. Viret, A. Anane, V. Cros, S. O. Demokritov, J. L. Prieto, M. Muñoz, G. de Loubens, and O. Klein, Full Control of the Spin_Wave Damping in a Magnetic Insulator Using Spin-Orbit Torque, Phys. Rev. Lett. **113**, 197203 (2014).

35. L. Liu, C.-F. Pai, D. C. Ralph, and R. A. Buhrman, Magnetic oscillations driven by the spin Hall effect in 3-terminal magnetic tunnel junction devices, Phys. Rev. Lett. **109**, 186602 (2012).

36. V. E. Demidov, S. Urazhdin, H. Ulrichs, V. Tiberkevich, A. Slavin, D. Baither, G. Schmitz, and S. O. Demokritov, Magnetic nano-oscillator driven by pure spin current, Nat. Mater. **11**, 1028 (2012).

37. R. H. Liu, W. L. Lim, and S. Urazdhin, Spectral characteristics of the microwave emission by the spin-Hall oscillator, Phys. Rev. Lett. **110**, 147601 (2013).

38. J. Sklenar, W. Zhang, M. B. Jungfleisch, W. Jiang, H. Chang, J. E. Pearson, M. Wu, J. B. Ketterson, and A. Hoffmann, Driving and detecting ferromagnetic resonance in insulators with the spin Hall effect, arXiv:1505.07791.

39. M. B. Jungfleisch, W. Zhang, J. Sklenar, J. Ding, W. Jiang, H. Chang, F. Y. Fradin, J. E. Pearson, J. B. Ketterson, V. Novosad, M. Wu, and A. Hoffmann, Large spin-

wave bullet in a ferromagnetic insulator driven by spin Hall effect, arXiv:1508.01427.

40. C. Hahn, G. de Loubens, O. Klein, M. Viret, V. V. Naletov, and J. Ben Youssef, Comparative measurements of inverse spin Hall effects and magnetoresistance, Phys. Rev. B **87**, 174417 (2013).

41. C. T. Boone, H. T. Nembach, J. M. Shaw, and T. J. Silva, Spin transport parameters in metallic multilayers determined by ferromagnetic resonance measurements of spin-pumping, J. Appl. Phys. **113**, 153906 (2013).

42. J.-C. Rojas-Sánchez, N. Reyren, P. Laczkowski, W. Savero, J.-P. Attané, C. Deranlot, M. Jamet, J.-M. George, L. Vila, and H. Jaffrès, Spin Pumping and Inverse Spin Hall Effect in Platinum: The Essential Role of Spin-Memory Loss at Metallic Interfaces, Phys. Rev. Lett. **112**, 106602 (2014).

43. W. Zhang, M. B. Jungfleisch, W. Jiang, J. Sklenar, F. Y. Fradin, J. E. Pearson, J. B. Ketterson, and A. Hoffmann, Spin pumping and inverse spin Hall effects – Insights for future spin-orbitronics (invited), J. Appl. Phys. **117**, 172610 (2015).

44. V. M. Edelstein, Spin polarization of conduction electrons induced by electric current in two-dimensional asymmetric electron systems, Solid State Commun. **73**, 233 (1990).

45. D. Culcer and R. Winkler, Generation of spin currents and spin densities in systems with reduced symmetry, Phys. Rev. Lett. **99**, 226601 (2007).

46. M. B. Jungfleisch, W. Zhang, J. Sklenar, W. Jiang, J. E. Pearson, J. B. Ketterson, and A. Hoffmann, Interface-driven spin-torque ferromagnetic resonance by

Rashba coupling at the interface between non-magnetic metals, arXiv:1508.01410.

47. A. Chernyshov, M. Overby, X. Liu, J. K. Furdyna, Y. Lyanda-Geller, and L. P. Rokhinson, Evidence for reversible control of magnetization in a ferromagnetic material by means of spin-orbit magnetic field, Nat. Phys. **5**, 656 (2009).

48. M. Z. Hasan and C. L. Kane, Colloquium: Topological insulators, Rev. Mod. Phys. **82**, 3045 (2010).

49. M. Z. Hasan and J. E. Moore, Three-dimensional topological insulators, Ann. Rev. Cond. Mat. Phys. **2**, 55 (2011).

50. C. H. Li, O. M. J. van 't Erve, J. T. Robinson, Y. Liu, L. Li, and B. T. Jonker, Electrical detection of charge-current-induced spin polarization due to spin-momentum locking in Bi_2Se_3, Nat. Nanotech. **9**, 218 (2014).

51. A. R. Mellnick, J. S. Lee, A. Richardella, J. L. Grab, P. J. Mintun, M. H. Fischer, A. Vaezi, A. Manchon, E.-A. Kim, N. Samarth, and D. C. Ralph, Spin-transfer torque generated by a topological insulator, Nature **511**, 449 (2014).

52. Y. Fan, P. Upadhyaya, X. Kou, M. Lang, S. Takei, Z. Wang, J. Tang, L. He, L.-T. Chang, M. Montazeri, G. Yu, W. Jiang, T. Nie, R. N. Schwartz, Y. Tserkovnyak, and K. L. Wang, Magnetization switching through giant spin-orbit torque in a magnetically doped topological insulator heterostructure, Nat. Mater. **13**, 699 (2014).

53. S. Mizukami, Y. Ando, and T. Miyazaki, Effect of spin diffusion on Gilbert damping for a very thin permalloy layer in Cu/permalloy/Cu/Pt films, Phys. Rev. B **66**, 104413 (2002).

54. B. Heinrich, Y. Tserkovnyak, G. Woltersdorf, A. Brataas, R. Urban, and G. E. W. Bauer, Dynamic exchange coupling in magnetic bilayers, Phys. Rev. Lett. **90**, 187601 (2003).

55. A. Azevedo, L. H. Vilela-Leão, R. L. Rodriguez-Suarez, A. B. Oliviera, and S. M. Rezende, DC effect in ferromagnetic resonance: Evidence of the spin-pumping effect?, J. Appl. Phys. **97**, 10C715 (2005).

56. E. Saitoh, M. Ueda, H. Miyajima, and G. Tatara, Conversion of spin current into charge current at room temperature: Inverse spin-Hall effect, Appl. Phys. Lett. **88**, 182509 (2006).

57. O. Mosendz, J. E. Pearson, F. Y. Fradin, G. E. W. Bauer, S. D. Bader, and A. Hoffmann, Quantifying spin Hall angles from spin pumping: Experiments and theory, Phys. Rev. Lett. **104**, 046601 (2010).

58. V. Vlaminck, J. E. Pearson, S. D. Bader, and A. Hoffmann, Dependence of spin-pumping spin Hall effect measurements on layer thicknesses and stacking order, Phys. Rev. B **88**, 064414 (2013).

59. O. Mosendz, V. Vlaminck, J. E. Pearson, F. Y. Fradin, G. E. W. Bauer, S. D. Bader, and A. Hoffmann, Detection and quantification of inverse spin Hall effect from spin pumping in permalloy/normal metal bilayers, Phys. Rev. B **82**, 214403 (2010).

60. G. Schmidt, D. Ferrand, L. W. Molenkamp, A. T. Filip, and B. J. van Wees, Fundamental obstacle for electrical spin injection from a ferromagnetic metal into a diffusive semiconductor, Phys. Rev. B **62**, R4790(R) (2000).

61. E. Shikoh, K. Ando, K. Kubo, E. Saitoh, T. Shinjo, and M. Shiraishi, Spin-Pump-Induced Spin Transport in *p*-Type Si at Room Temperature, Phys. Rev. Lett. **110**, 127201 (2013).

62. K. Ando, S. Takahashi, J. Ieda, H. Kurebayashi, T. Trypiniotis, C. H. W. Barnes, S. Maekawa, and E. Saitoh, Electrically tunable spin injector free from the impedance mismatch problem, Nat. Mater. **10**, 655 (2011).

63. S. Watanabe, K. Ando, K. Kang, S. Mooser, Y. Vaynzof, H. Kurebayashi, E. Saitoh, and H. Sirringhaus, Polaron spin current transport in organic semiconductors, Nat. Phys. **10**, 308 (2014).

64. Z. Tang, E. Saitoh, H. Ago, K. Kawahara, Y. Ando, T. Shinjo, and M. Shiarishi, Dynamically generated pure spin current in single-layer graphene, Phys. Rev B **87**, 140401(R) (2013).

65. Y. Shiomi, K. Nomura, Y. Kajiwara, K. Eto, M. Novak, K. Segawa, Y. Ando, and E. Saitoh, Spin-Electricity Conversion Induced by Spin Injection into Topological Insulators, Phy. Rev. Lett. **113**, 196601 (2014).

66. A. A. Baker, A. I. Fugueroa, L. J. Collins-McIntyre, G. van der Laan, and T. Hesdedal, Spin pumping in Ferromagnet-Topological Insulator-Ferromagnet Heterostructures, Sci. Rep. **5**, 7907 (2015).

67. J.-C. Rojas Sánchez, L. Vila, G. Desfonds, S. Gambarelli, J. P. Attane, J. M. De Teresa, C. Magén, and A. Fert, Spin-to-charge conversion using

Rashba coupling at the interface between non-magnetic materials, Nat. Comm. **4**, 2944 (2013).

68. W. Zhang, M. B. Jungfleisch, W. Jiang, J. E. Pearson, and A. Hoffmann, Spin pumping and inverse Rashba-Edelstein effect in NiFe/Ag/Bi and NiFe/Ag/Sb, J. Appl. Phys. **117**, 17C727 (2015).

69. H. Wang, C. Du, P. C. Hammel, and F. Yang, Antiferromagnonic Spin Transport from $Y_3Fe_5O_{12}$ into NiO, Phys. Rev. Lett. **113**, 097202 (2014).

70. I. Dzyaloshinsky, A thermodynamic theory of "weak" ferromagnetism of antiferromagnetics, J. Phys. Chem. Solids **4**, 241 (1958).

71. T. Moriya, Anisotropic Superexchange Interaction and Weak Ferromagnetism, Phys. Rev. **120**, 91 (1960).

72. M. Bode, M. Heide, K. von Bergmann, P. Ferriani, S. Heinze, G. Bihlmayer, A. Kubetzka, O. Pietzsch, S. Blügel, and R. Wiesendanger, Chiral magnetic order at surfaces driven by inversion asymmetry, Nature **447**, 190 (2007).

73. G. Chen, T. P. Ma, A. T. N'Diaye, H. Kwon, C. Won, Y. Z. Wu, and A. K. Schmid, Tailoring the chirality of magnetic domain walls by the interface engineering, Nat. Comm. **4**, 3671 (2013).

74. G. Chen, J. Zhu, A. Quesada, J. Li, A. T. N'Diaye, Y. Huo, T. P. Ma, Y. Chen, H. Y. Kwon, C. Won, Z. Q. Qiu, A. K. Schmid, and Y. Z. Wu, Novel Chiral Magnetic Domain Wall Structure in Fe/Ni/Cu(001) Films, Phys. Rev. Lett. **110**, 177204 (2013).

75. S. Emori, U. Bauer, S. M. Ahn, E. Martinez, and G. S. D. Beach, Current-driven dynamics of chiral ferromagnetic domain walls, Nat. Mater. **12**, 611 (2013).

76. K. S. Ryu, L. Thomas, S. H. Yang, and S. Parkin, Chiral spin torque at magnetic domain walls, Nat. Nanotech. **8**, 527 (2013).

77. O. Boulle, S. Rohart, L. D. Buda-Prejbeanu, E. Jue, I. M. Miron, S. Pizzini, J. Vogel, G. Gaudin, and A. Thiaville, Domain Wall Tilting in the Presence of the Dzyalosjinskii-Moriya Interaction in Out-of-Plane Magnetized Magnetic Nanotracks, Phys. Rev. Lett. **111**, 217203 (2013).

78. S. Emori, E. Martinez, K.-J. Lee, H.-W. Lee, U. Bauer, S. M. Ahn, P. Agrawal, D. C. Bono, and G. S. D. Beach, Spin Hall torque magnetometry of Dzyaloshinskii domain walls, Phys. Rev. B **90**, 184427 (2014).

79. S.-H. Yang, K.-S. Ryu, and S. Parkin, Domain-wall velocities of up to 750 m s^{-1} driven by exchange coupling torque in synthetic antiferromagnets, Nat. Nanotech. **10**, 221 (2015).

80. S. S. P. Parkin, M. Hayashi, and L. Thomas, Magnetic domain-wall racetrack memory, Science **320**, 190 (2008).

81. S. Heinze, K. von Bergmann, M. Menzel, J. Brede, A. Kubetzka, R. Wisendanger, G. Bihlmayer, and S. Blügel, Spontaneous atomic-scale magnetic skyrmion lattice in two dimensions, Nat. Phys. **7**, 713 (2011).

82. N. Romming, C. Hanneken, M. Menzel, J. E. Bickel, B. Wolter, K. von Bergmann, A. Kubetzka, and R. Wiesendanger, Writing and Deleting Single Magnetic Skyrmions, Science **341**, 636 (2013).

83. F. Büttner, C. Moutafis, M. Schneider, B. Krüger, C. M. Günther, J. Gellhufe, C. v. Korff Schmising, J. Mohanty, B. Pfau, S. Schaffert, A. Bisig, M. Foerster, T. Schulz, C. A. F. Vaz, J. H. Franken, H. J. M. Swagten, M. Kläui, and S. Eisebitt,

Dynamics and inertia of skyrmionic spin structures, Nat. Phys. **11**, 225 (2015).

84. W. Jiang, P. Upadhyaya, W. Zhang, G. Yu, M. B. Jungfleisch, F. Y. Fradin, J. E. Pearson, Y. Tserkovnyak, K. L. Wang, O. Heinonen, S. G. E. te Velthuis, and A. Hoffmann, Blowing Magnetic Skyrmion Bubbles, Science **349**, 283 (2015).

85. C. Moreau-Luchaire, C. Moutafis, N. Reyren, J. Sampaio, N. Van Horne, C. A. F. Vaz, K. Bouzehouane, K. Garcia, C. Deranlot, P. Warnicke, P. Wohlhüter, J.-M. George, M. Wigand, J. Raabe, V. Cros, and A. Fert, Skyrmions at room temperature: From magnetic thin films to magnetic multilayers, ArXiv:1502.07853.

86. S. Woo, K. Litzius, B. Krüger, M.-Y. Im, L. Caretta, K. Richter, M. Mann, A. Krone, R. Reeve, M. Weigand, P. Agrawal, P. Fischer, M. Kläui, and G. S. D. Beach, Observation of room temperature magnetic skyrmions and their current-driven dynamics in ultrathin Co films, ArXiv:1502.07376.

87. S. Mühlbauer, B. Binz, F. Jonietz, C. Pfleiderer, A. Rosch, A. Neubauer, R. Georgii, and P. Böni, Skyrmion Lattice in a Chiral Magnet, Science **323**, 915 (2009).

88. T. H. R. Skyrme, A unified field theory of mesons and baryons, Nucl. Phys. **31**, 556 (1962).

89. A. Bogdanov and A. Yablonskii, Thermodynamically stable "vortices" on magnetically ordered crystals, JETP Lett. **68**, 101 (1989).

90. H.-B. Braun, Topological effects in nanomagnetism: from superparamagnetism to chiral quantum solitons, Adv. Phys. **61**, 1 (2012).

91. N. Nagaosa and Y. Tokura, Topological properties and dynamics of magnetic skyrmions, Nat. Nanotech. **8**, 899 (2013).

92. E. Ruff, S. Widmann, P. Lunkenheimer, V. Tsurkan, S. Bordács, I. Kézsmárki, and A. Loidl, Ferroelectric Skyrmions and a Zoo of Multiferroic Phases in GaV_4S_8, ArXiv:1504.00309.

93. L. Sun, R. X. Cao, B. F. Miao, Z. Feng, B. You, D. Wu, W. Zhang, A. Hu, and H. Ding, Creating and Artificial Two-Dimensional Skyrmion Crystal by Nanopatterning, Phys. Rev. Lett. **110**, 167201 (2013).

94. B. F. Miao, L. Sun, Y. W. Wu, X. D. Tao, X. Xiong, Y. Wen, R. X. Cao, P. Wang, D. Wu, Q. F. Zhan, B. You, J. Du, R. W. Li, and H. F. Ding, Experimental realization of two-dimensional artificial skyrmion crystals at room temperature, Phys. Rev. B **90**, 174411 (2014).

95. Y. Tokunaga, X. Z. Yu, J. S. White, H. M. Rønnow, D. Morikawa, Y. Taguchi, and Y. Tokura, A new class of chiral materials hosting magnetic skyrmions beyond room temperature, Nature Comm. **6**, 7638 (2015).

96. A. Neubauer, C. Pfleiderer, B. Binz, A. Rosch, R. Ritz, P. G. Niklowitz, and P. Böni, Topological Hall Effect in the *A* Phase of MnSi, Phys. Rev. Lett. **102**, 186602 (2009).

97. K. Everschor-Sitte and M. Sitte, Real-space Berry phases: Skyrmion soccer (invited), J. Appl. Phys. **115**, 172602 (2014).

98. T. Schulz, R. Ritz, A. Bauer, M. Halder, M. Wagner, C. Franz, C. Pfleiderer, K. Everschor, M. Garst, and A. Rosch, Emergent electrodynamics of skyrmions in a chiral magnet, Nat. Phys. **8**, 301 (2012).

99. A. Fert, V. Cros, and J. Sampaio, Skyrmions on the track, Nat. Nanotech. **8**, 152 (2013).

100. J. Eggers, Nonlinear dynamics and breakup of free-surface flows, Rev. Mod. Phys. **69**, 865 (1997).

101. Z. Q. Qiu and S. D. Bader, Surface magneto-optic Kerr effect (SMOKE), J. Magn. Magn. Mater. **200**, 664 (1999).

102. K.-W. Moon, D.-H. Kim, S.-C. Yoo, S.-G. Je, B. S. Chun, W. Kim, B.-C. Min, C. Hwang, and S.-B. Choe, Magnetic bubblecade memory based on chiral domain walls, Sci. Rep. **5**, 9166 (2015).

103. G. E. W. Bauer, E. Saitoh, and B. J, van Wees, Spin caloritronics, Nat. Mater. **11**, 391 (2012).

104. K. Uchida, S. Takahashi, K. Harii, J. Ieda, W. Koshibae, K. Ando, S. Maekawa, and E. Saitoh, Observation of the spin Seebeck effect, Nature **455**, 778 (2008).

105. K. Uchida, J. Xiao, H. Adachi, J. Ohe, S. Takahashi, J. Ieda, T. Ota, Y. Kajiwara, H. Umezawa, H. Kawai, G. E. W. Bauer, S. Maekawa, and E. Saitoh, Spin Seebeck Insulator, Nat. Mater. **9**, 894 (2010).

106. K. Uchida, H. Adachi, T. Ota, H. Nakayama, S. Maekawa, and E. Saitoh, Observation of longitudinal spin-Seebeck effect in magnetic insulators, Appl. Phys. Lett. **97**, 172505 (2010).

107. C. M. Jaworski, J. Yang, S. Mack, D. D. Awschalom, J. P. Heremans, and R. C. Myers, Observation of the spin Seebeck effect in a ferromagnetic semiconductor, Nat. Mater. **9**, 893 (2010).

108. C. M. Jaworski, J. Yang, S. Mack, D. D. Awschalom, R. C. Myers, and J. P. Heremans, Spin-Seebeck Effect: A Phonon Driven Spin Distribution, Phys. Rev. Lett. **106**, 186601 (2011).

109. S. Y. Huang, W. G. Wang, S. F. Lee, J. Kwo, and C. L. Chien, Intrinsic Spin-Dependent Thermal Transport, Phys. Rev. Lett. **107**, 216604 (2011).

110. A. D. Avery, M. R. Pufall, and B. L. Zink, Observation of the Planar Nerst Effect in Permalloy and Nickel Thin Films with In-Plane Thermal Gradients, Phys. Rev. Lett. **109**, 196602 (2012).

111. M. Schmid, S. Srichandan, D. Meier, T. Kuschel, J.-M. Schmalhorst, M. Vogel, G. Reiss, C. Strunk, and C. H. Back, Transverse Spin Seebeck Effect versus Anomalous and Planar Nernst Effects in Permalloy Thin Films, Phys. Rev. Lett. **111**, 187201 (2013).

112. D. Qu, S. Y. Huang, J. Hu, R. Wu, and C. L. Chien, Intrinsic Spin Seebeck Effect in Au/YIG, Phys. Rev. Lett. **110**, 067206 (2013).

113. T. Kikkawa, K. Uchida, S. Daimon, Y. Shiomi, H. Adachi, Z. Qiu, D. Hou, X.-F. Jin, S. Maekawa, and E. Saitoh, Separation of longitudinal spin Seebeck effect from anomalous Nernst effect: Determination of origin of transverse thermoelectric voltage in metal/insulator junctions, Phys. Rev. B **88**, 214403 (2013).

114. S. M. Wu, J. Hoffman, J. E. Pearson, and A. Bhattacharya, Unambiguous separation of the inverse spin Hall and anomalous Nernst effects with a ferromagnetic metal using the spin Seebeck effect, Appl. Phys. Lett. **105**, 092409 (2014).

115. M. Weiler, M. Althammer, F. D. Czeschka, H. Huebl, M. S. Wagner, M. Opel, I.-M. Imort, G. Reiss, A. Thomas, R. Gross, and S. T. B. Goennenwein, Local Charge and Spin Currents in Magnetothermal Landscapes, Phys. Rev. Lett. **108**, 106602 (2012).

116. M. Schreier, N. Roschewsky, E. Dobler, S. Meyer, H. Huebl, R. Gross, and S. T. B. Goennewein, Current heating induced spin Seebeck effect, Appl. Phys. Lett. **103**, 242402 (2013).

117. S. M. Wu, F. Y. Fradin, J. Hoffman, A. Hoffmann, and A. Bhattacharya, Spin Seebeck devices using local on-chip heating, J. Appl. Phys. **117**, 17C509 (2015).

118. J. Xiao, G. E. W. Bauer, K. Uchida, E. Saitoh, and S. Maekawa, Theory of magnon-driven spin Seebeck effect, Phys. Rev B **81**, 214418 (2010).

119. M. Schreier, A. Kamra, M. Weiler, J. Xiao, G. E. W. Bauer, R. Gross, and S. T. B. Goennenwein, Magnon, phonon, and electron temperature profiles and the spin Seebck effect in magnetic insulator/normal metal hybrid structures, Phys. Rev. B **88**, 094410 (2013).

120. S. Hoffman, K. Sato, and Y. Tserkovnyak, Landau-Lifshitz theory of the longitudinal spin Seebeck effect, Phys. Rev. B **88**, 064408 (2013).

121. S. M. Rezende, R. L. Rodríguez-Suárez, R. O. Cunha, A. R. Rodrigues, F. L. A. Machado, G. A. Fonseca Guerra, J. C. Lopez Ortiz, and A. Azevedo, Magnon spin-current theory for the longitudinal spin-Seebeck effect, Phys. Rev. B **89**, 014416 (2014).

122. J. Flipse, F. K. Dejene, D. Wagenaar, G. E. W. Bauer, J. Ben Youssef, and B. J. van Wees, Observation of the Spin Peltier Effect for Magnetic Insulators, Phys. Rev. Lett. **113**, 027601 (2014).

123. A. Slachter, F. L. Bakker, J. P. Adam, and B. J. van Wees, Thermally driven spin injection from a ferromagnet into a non-magnetic metal, Nat. Phys. **6**, 879 (2010).

124. J. Flipse, F. L. Bakker, A. Slachter, F. K. Dejene, and B. J. van Wees, Direct observation of the spin-dependent Peltier effect, Nat. Nanotech. **7**, 166 (2012).

125. T. An, V. I. Vasyuchka, K. Uchida, A. V. Chumak, K. Yamaguchi, K. Harii, J. Ohe, M. B. Jungfleisch, Y. Kajiwara, H. Adachi, B. Hillebrands, S. Maekawa, and E. Saitoh, Unidirectional spin-wave heat conveyer, Nat. Mater. **12**, 549 (2013).

126. J. Brüggemann, S. Weiss, P. Nalbach, and M. Thorwart, Cooling a Magnetic Nanoisland by Spin-Polarized Currents, Phys. Rev. Lett. **113**, 076602 (2014).

127. A. Kirihara, K. Uchida, Y. Kajiwara, M. Ishida, Y. Nakamura, T. Manako, E. Saitoh, and S. Yorozu, Spin-current driven thermoelectric coating, Nat. Mater. **11**, 686 (2012).

128. A. B. Cahaya, O. A. Tretiakov, and G. E. W. Bauer, Spin Seebeck power generators, Appl. Phys. Lett. **104**, 042402 (2014).

129. J. C. Slonczewski, Initiation of spin-transfer torque by thermal transport from magnons, Phys. Rev. B **82**, 054403 (2010).

130. D. Hinzke and U. Nowak, Domain Wall Motion by the Magnonic Spin Seebeck Effect, Phys. Rev. Lett. **107**, 027205 (2011).

131. A. A. Kovalev and Y. Tserkovnyak, Thermomagnonic spin transfer and Peltier effects in insulating magnets, Europhys. Lett. **97**, 67002 (2012).

132. L. Kong and J. Zang, Dynamics of an Insulating Skyrmion under a Temperature Gradient, Phys. Rev. Lett. **111**, 067203 (2013).

133. W. Jiang, P. Upadhyaya, Y. Fan, J. Zhao, M. Wang, L.-T. Chang, M. Lang, K. L. Wong, M. Lewis, Y.-T. Lin, J. Tang, S. Cherepov, X. Zhou, Y. Tserkovnyak, R. N. Schwartz, and K. L. Wang, Direct Imaging of Thermally Driven Domain Wall Motion in Magnetic Insulators, Phys. Rev. Lett. **110**, 177202 (2013).

134. M. Mochizuki, X. Z. Yu, S. Seki, N. Kanazawa, W. Kochibae, J. Zang, M. Mostovoy, Y. Tokura, and N. Nagaosa, Thermally driven ratchet motion of a skyrmion microcrystal and topological magnon Hall effect, Nat. Mater. **13**, 241 (2014).

135. D. Qu, S. Y. Huang, B. F. Miao, S. X. Huang, and C. L. Chien, Self-consistent determination of spin Hall angles in selected 5d metals by thermal spin injection, Phys. Rev. B **89**, 140407(R) (2014).

136. H. Schultheiss, J. E. Pearson, S. D. Bader, and A. Hoffmann, Thermoelectric detection of spin waves, Phys. Rev. Lett. **109**, 237204 (2012).

137. Recent Advances in Magnetic Insulators – From Spintronics to Microwave Applications, edited by M. Wu and A. Hoffmann, Solid State Physics **64**, (Academic Press, 2013).

138. V. V. Kruglyak, S. O. Demokritov, and D. Grundler, Magnonics, J. Phys. D: Appl. Phys. **43**, 264001 (2010).

139. A. A. Serga, A. V. Chumak, and B. Hillebrands, YIG magnonics, J. Phys. D: Appl. Phys. **43**, 264002 (2010).

140. B. Lenk, H. Ulrichs, F. Garbs, and M. Münzenberg, The building blocks of magnonics, Phys. Rep. **507**, 107 (2011).

141. T. Schneider, A. A. Serga, B. Leven, B. Hillebrands, R. L. Stamps, and M. P. Kostylev, Realization of spin-wave logic gates, Appl. Phys. Lett. **92**, 022505 (2008).

142. F. Macià, F. C. Hoppensteadt, and A. D. Kent, Spin wave excitation patterns generated by spin torque oscillators, Nanotechn. **25**, 045303 (2014).

143. B. Obry, T. Meyer, P. Pirro, T. Brächer, B. Lägel, J. Osyen, T. Strache, J. Fassbender, and B. Hillebrands, Microscopic magnetic structuring of a spin-wave waveguide by ion implantation in a $Ni_{81}Fe_{19}$ layer, Appl. Phys. Lett. **102**, 022409 (2013).

144. K. Vogt, H. Schultheiss, S. Jain, J. E. Pearson, A. Hoffmann, S. D. Bader, and B. Hillebrands, Spin waves turning a corner, Appl. Phys. Lett. **101**, 042410 (2012).

145. K. Vogt, F. Y. Fradin, J. E. Pearson, S. D. Bader, T. Sebastian, B. Hillebrands, A. Hoffmann, and H. Schultheiss, Realization of a spin-wave multiplexer, Nat. Comm. **5**, 3727 (2014).

146. A. V. Chumak, A. A. Serga, and B. Hillebrands, Magnon transistor for all-magnon data processing, Nat. Comm. **5**, 4700 (2014).

147. S. O. Demokritov, V. E. Demidov, O. Dzyapko, G. A. Melkov, A. A. Serga, B. Hillebrands, and A. N. Slavin, Bose-Einstein condensation of quasi-equilibrium magnons at room temperature under pumping, Nature **443**, 430 (2006).

148. P. Nowik-Boltyk, O. Dzyapko, V. E. Demidov, N. G. Berloff and S. O. Demokritov, Spatially non-uniform ground state and quantized vortices in a two-component Bose-Einstein condensate of magnons, Sci. Rep. **2**, 482 (2012).

149. J. König, M. Chr. Bønsager, and A. H. MacDonald, Dissipationless spin transport in thin film ferromagnets, Phys. Rev. Lett. **87**, 187202 (2001).

150. S. Takei and Y. Tserkovnyak, Superfluid spin transport through easy-plane ferromagnetic insulators, Phys. Rev. Lett. **112**, 272701 (2014).

151. H. Chen, A. D. Kent, A. H. MacDonald, and I. Sodemann, Nonlocal transport mediated by spin supercurrents, Phys. Rev. B **90**, 220401 (2014).

152. P. Clausen, D. A. Bozhko, V. I. Vasyuchka, G. A. Melkov, B. Hillebrands, and A. A. Serga, Magnon supercurrent in a magnon Bose-Einstein condensate subject to a thermal gradient, arXiv:1503.00482.

153. K. Nakata, K. A. van Hoogdalem, P. Simon, and D. Loss, Josephson and persistent spin currents in Bose-Einstein condensates of magnons, Phys. Rev. B **90**, 144419 (2014).

154. R. Huber and D. Grundler, Ferromagnetic nanodisks for magnonic crystals and waveguides, Proc. of SPIE **8100**, 8100D (2011).

155. S. Tacchi, F. Montoncello, M. Madami, G. Gubbiotti, G. Carlotti, L. Giovannini, R. Zivieri, F. Nizzoli, S. Jain, A. O. Adeyeye, and N. Singh, Band diagram of spin waves in a two-dimensional magnonic crystal, Phys. Rev. Lett. **107**, 127204 (2011).

156. R. Shindou, J. Ohe, R. Matsumoto, S. Murakami, and E. Saitoh, Chiral spin-wave edge modes in dipolar magnetic thin films, Phys. Rev. B **87**, 174402 (2013).

157. R. Shindou, R. Matsumoto, S. Murakami, and J. Ohe, Topological chiral magnonic edge mode in a magnonic crystal, Phys. Rev. B **87**, 174427 (2013).

158. T. Shinjo, T. Okuno, R. Hassdorf, K. Shigeto, and T. Ono, Magnetic vortex core observation in circular dots of permalloy, Science **289**, 930 (2000).

159. J. P. Park, P. Eames, D. M. Engebretson, J. Berzovsky, and P. A. Crowell, Imaging of spin dynamics in closure domains and vortex structures, Phys. Rev. B **67**, 020403 (2003).

160. V. Novosad, F. Fradin, P. Roy, K. Buchanan, K. Guslienko, and S. D. Bader, Magnetic vortex resonance in patterned ferromagnetic dots, Phys. Rev. B **72**, 024455 (2005).

161. B. Waeyenberge, A. Puzic, H. Stoll, K. W. Chou, T. Tyliszczak, R. Hertel, M. Fähnle, H. Brückl, K. Rott, G. Reiss, I. Neudecker, D. Weiss, C. H. Back, and G. Schütz, Magnetic vortex core reversal by excitation with short bursts of an alternating field, Nature **444**, 461 (2006).

162. J. Shibata, K. Shigeto, and Y. Otani, Dynamics of magnetostatically coupled vortices in magnetic nanodisks, Phys. Rev. B **67**, 224404 (2003).

163. K. S. Buchanan, P. E. Roy, M. Grimsditch, F. Y. Fradin, K. Y. Guslienko, S. D. Bader, and V. Novosad, Soliton pair dynamics in patterned ferromagnetic ellipses, Nat. Phys. **1**, 172 (2005).

164. J. Shibata and Y. Otani, Magnetic vortex dynamics in a two-dimensional square lattice of ferromagnetic nanodisks, Phys. Rev. B **70**, 012404 (2004).

165. Persistent Spectral Hole Burning: Science and Applications, edited by W. E. Moerner (Springer, Berlin, 1988).

166. C. F. Adolff, M. Hänze, A. Vogel, M. Weigand, M. Martens, and G. Meier, Self-organized state formation in magnonic vortex crstals, Phys. Rev. B **88**, 224425 (2013).

167. M. Hänze, C. F. Adolff, M. Weigand, and G. Meier, Burst-mode manipulation of magnonic vortex crystals, Phys. Rev. B **91**, 104428 (2015).

168. S. Gliga, A. Kákay, R. Hertel, and O. G. Heinonen, Spectral Analysis of Topological Defects in an Artificial Spin-Ice Lattice, Phys. Rev. Lett. **110** 117205 (2013).

169. C. Mead, Neuromorphic Electronic Systems, Proc. IEEE **78**, 1629 (1990).

170. A. Imre, C. Csaba, l. Ji, A. Olrlov, G. H. Bernstein, and W. Porod, Majority Logic Gate for Magnetic Quantum-Dot Cellular Automata, Science **311**, 205 (2006).

171. A. A. Khajetoorians, J. Wiebe, B. Chilian, and R. Wiesendanger, Realizing All-Spin-Based Logic Operations Atom by Atom, Science **332**, 1062 (2011).

172. S. Jain, V. Novosad, F. Y. Fradin, J. E. Pearson, V.Tiberkevich, A. N. Slavin, and S. D. Bader, From chaos to selective ordering of vortex cores in interacting mesomagnets, Nat. Comm. **3**, 1330 (2012).

173. K- Zhao, Q. Zhang, M. Chini, Y. Wu, X. Wang, and Z. Chang, Tailoring a 67 attosecond pulse through advantageous phase-mismatch, Optics Letts. **37**, 3891 (2012).

174. L. Young, E. P. Kanter, B. Krässig, Y. Li, A. M. March, S. T. Pratt, R. Santra, S. H. Southworth, N. Rohringer, L. F. DiMauro, G. Doumy, C. A. Roedig, N. Berrah, L. Fang, M. Hoener, P. H. Bucksbaum, J. P. Sryan, S. Ghimire, J. M. Glowina, D. A. Riess, J. D. Bozed, C. Bostedt, and M. Messerschmidt, Femtosecond electronic response of atoms to ultra-intense X-rays, Nature **466**, 56 (2010).

175. A. Scholl, L. Baumgarten, R. Jacquemin, and W. Eberhardt, Ultrafast Spin Dynamics of Ferromagnetic Thin Films Observed by fs Spin-Resolved Two-Photon Photoemission Phys. Rev. Lett. **79**, 5146 (1997).

176. R. Carley, K. Döbrich, B. Frietsch, C. Gahl, M. Teichmann, O. Schwarzkopf, P. Wernet, and M. Weinelt, Femtosecond Laser Excitation Drives Ferromagnetic Gadolinium out of Magnetic Equilibrium, Phys. Rev. Lett. **109**, 057401 (2012).

177. C. D. Stanciu, A. Tsukamoto, A. V. Kimel, F. Hansteen, A. Kirilyuk, A. Itoh, and Th. Rasing, Subpicosecond Magnetization Reversal across Ferrimagnetic Compensation Points, Phys. Rev. Lett. **99,** 217204 (2007) .

178. G. Malinowski, F. Dalla Longa, J. H. H. Rietjens, P. V. Paluskar, R. Huijink, H. J. M. Swagten, and B. Koopmans, Control of speed and efficiency of ultrafast demagnetization by direct transfer of spin angular momentum, Nat. Phys. **4** 855 (2008).

179. B. Koopmans, G. Malinowski, F. Dalla Longa, D. Steiauf, M. Fähnle, T. Roth, M. Cinchetti, and M. Aeschlimann, Explaining the paradoxical diversity of ultrafast laser-induced demagnetization, Nat. Matls. **9**, 259 (2010).

180. H. B. Zhao, D. Talbayev, X. Ma, Y. H. Ren, A. Venimadhav, Qi Li, and G. Lüpke, Coherent Spin Precession via Photoinduced Antiferromagnetic Interactions in $La_{0.67}Ca_{0.33}MnO_{3,}$ Phys. Rev. Lett. **107**, 207205 (2011).

181. E.Turgut, C. La-o-vorakiat, J. M. Shaw, P. Grychtol, H. T. Nembach, D. Rudolf, R. Adam, M. Aeschlimann, C M. Schneider, T. J. Silva, M. M. Murnane, H. C. Kapteyn, and S. Mathias, Controlling the Competition between Optically Induced Ultrafast Spin-Flip Scattering and Spin Transport in Magnetic Multilayers, Phys. Rev. Lett. **110**, 197201 (2013).

182. P. M. Oppeneer and A. Liebsch, Ultrafast demagnetization in Ni: theory of magneto-optics for non-equilibrium electron distributions, J. Phys.: Cond. Matt. **16** 5519 (2004).

183. K. Carva, M. Battiato, and P. M. Oppeneer, *Ab Initio* Investigation of the Elliott-Yafet Electron-Phonon Mechanism in Laser-Induced Ultrafast Demagnetization, Phys. Rev. Lett. **107**, 207201 (2011).

184. E. Beaurepaire, J.-C. Merle, A. Daunois, and J.-Y. Bigot, Ultrafast Spin Dynamics in Ferromagnetic Nickel, Phys. Rev. Lett. **76**, 4250 (1996).

185. H. C. Siegmann, E. L. Garwin, C. Y. Prescott, J. Heidmann, D. Mauri, D. Weller, R. Allenspach, and W. Weber, Magnetism with picosecond field pulses, J. Magn. Magn. Mater. **151**, L8 (1995).

186. C. H. Back, D. Weller, J. Heidmann, D. Mauri, D. Guarisco, E. L. Garwin, and H. C. Siegmann, Magnetization reversal in ultrashort magnetic field pulses, Phys. Rev. Lett. **81**, 3251 (1998).

187. J. Stöhr, and H. C. Siegmann, *Magnetism: From Fundamentals to Nanoscale Dynamics,* (Springer, Berlin) 2006.

188. A. Kirilyuk, A. V. Kimel, and T. Rasing, Ultrafast optical manipulation of magnetic order, Rev. Mod. Phys. **82**, 2731 (2010).

189. A. Kirilyuk, A. V. Kimel, and T. Raising, Laser-induced magnetization dynamics and reversal in ferrimagnetic alloys, Rep. Prog. Phys. **76**, 026501 (2013)**.**

190. I. Radu, K. Vahaplar, C. Stamm, T. Kachel, N. Pontius, H. A. Dürr, T. A. Ostler, J. Barker, R. F. L. Evans, R. W. Chantrell, A. Tsukamoto, A. Itoh, A. Kirilyuk, Th. Rasing, and A. V. Kimel, Transient ferromagnetic-like state mediating ultrafast reversal of antiferromagnetically coupled spins, Nature **472,** 205 (2011).

191. T. A. Ostler, J. Barker, R. F. L. Evans, R. W. Chantrell, U. Atxitia, O. Chubykalo-Fesenko, S. El Moussaoui, L. Le Guyader, E. Mengotti, L. J. Heyderman, F. Nolting, A. Tsukamoto, A. Itoh, D. Afanasiev, B. A. Ivanov, A. M. Kalashnikova, K. Vahaplar, J. Mentink A. Kirilyuk, Th. Rasing, and A. V. Kimel, Ultrafast heating as a sufficient stimulus for magnetization reversal in a ferromagnet*,* Nature Commun. **3**, 666 (2012).

192. S. Mangin, M. Gottwald, C.-H. Lambert, D. Steil, V. Uhlíř, L. Pang, M. Hehn, S. Alebrand, M. Cinchetti, G. Malinowski, Y. Fainman, M. Aeschlimann and

E. E. Fullerton, Engineered materials for all-optical helicity-dependent magnetic switching , Nat. Mater. **13**, 286 (2014).

193. C.-H. Lambert, S. Mangin, B. S. D. Ch. S. Varaprasad, Y. K. Takahashi, M. Hehn, M. Cinchetti, G. Malinowski, K. Hono, Y. Fainman, M. Aeschlimann, and E. E. Fullerton, All-optical control of ferromagnetic thin films and nanostructures, Science **345**, 1337 (2014).

194. S. S. P. Parkin, Systematic variation of the strength and oscillation period of indirect magnetic exchange coupling through the 3*d*, 4*d*, and 5*d* transition metals, Phys. Rev. Lett. **67**, 3598 (1991).

195. C. Mack, The Multiple Lives of Moore's Law, IEEE Spectrum **52**(4), 31 (2015).